A DISCRETE ELEMENT STUDY OF THE UNIAXIAL COMPRESSIVE RESPONSE OF PLAIN CONCRETE USING THE JCFPM CONSTITUTIVE MODEL

by

Anay Narendra Joshi

A thesis submitted to the faculty of
The University of North Carolina at Charlotte
in partial fulfillment of the requirements
for the degree of Master of Science in
Mechanical Engineering

Charlotte

2018

Approved by:

Dr. Harish P. Cherukuri

Dr. Miguel A. Pando

Dr. Ronald E. Smelser

ABSTRACT

ANAY NARENDRA JOSHI. A Discrete Element Study of the Uniaxial Compressive Response of Plain Concrete using the JCFPM Constitutive Model. (Under the direction of DR. HARISH P. CHERUKURI AND DR. MIGUEL A. PANDO)

The standard bonded-particle models available in many discrete element method (DEM) codes are known to predict unrealistically low values for the ratio of ultimate compressive strength (UCS) to tensile strength (UTS) for concrete. To correct this, various modifications to the bonded particle models or new constitutive laws have been proposed by various researchers. One of these is the Jointed Cohesive Frictional Particle Model (JCFPM) that introduced a parameter called the interaction range to account for high UCS to UTS ratios. In this work, JCFPM model is used to model the response of concrete under uniaxial compressive loading. A parametric study is carried out to study the effect that various DEM parameters such as the cohesion, packing density, particle generation methods and the interaction range have on the response of the concrete cylinder. Based on these studies, a calibrated DEM model that predicts results in agreement with the experimentally observed results is presented.

ACKNOWLEDGEMENTS

This thesis work is the output of efforts and assistance of many individuals. I would like to express my sincere gratitude to those who supported me technically and emotionally throughout the process. Without their help this work would not have been possible.

First, I wish to express my sincere gratitude towards my research advisors, Dr. Harish Cherukuri and Dr. Miguel Pando for their wholehearted guidance and encouragement throughout the duration of this work. I would like to express my gratitude to Dr. Cherukuri for the wealth of knowledge about Discrete Element Method he made available for this research. I would also like to thank Dr. Pando for his knowledge and experience in the field of Geomechanics. His inputs and efforts for this work are equally valuable to me. I would also like to thank Dr. Ronald Smelser for agreeing to serve on my thesis committee.

I would like to thank my search group for their constant help with even smallest technical difficulties I faced during the time. I would like to express my gratitude towards UNCC MOSAIC technical support team, especially Mr. Jason Edgecombe and Mr. Jason Jansen for their valuable support with application and computing difficulties. This work would not have been completed without their help. I would also like to mention Dr. Scholtès for his timely guidance regarding Yade software and subroutine script for it. I am thankful to Dr. Scholtѕ for offering his knowledge, expertise and experience in the implementation of the current model.

I would like to thank my parents Dr. Bhavna Joshi and Mr. Narendra Joshi for their valuable inputs to my work and emotional support throughout the process. I would like to mention here some of my friends Ms. Seva Shinde, Mr. Manish Patil, Mr. Amol Sathe, Mr. Jaydeep Kshirsagar and Ms. Ankita Paranjpe who constantly supported me and provided with their views, encouragement and expertise where ever applicable in my work. And lastly, I would like to express my gratitude towards my

family who has been very supportive and stood behind me in all the stages of this research work.

TABLE OF CONTENTS

LIST OF FIGURES

LIST OF TABLES

LIST OF ABBREVIATIONS

ΔD	Relative displacement between interacting discrete element particles
Δu_s	Shear displacement of particles
γ	Interaction range coefficient
ν	Poisson's ratio
ϕ	Friction angle
σ_c	Compressive strength
σ_t	Tensile strength
ζ	Softening factor
A_{int}	Interacting surface area
c	Cohesion
E	Modulus of elasticity
E_{eq}	Equivalent bulk modulus
F_n	Normal force
F_s	Shear force
k_n	Contact normal stiffness
k_s	Contact shear stiffness
t	Contact tensile strength
DE	Discrete Element
DEM	Discrete Element Method
JCFPM	Jointed Cohesive Friction Particle Model
UCS	Ultimate Compressive Strength

CHAPTER 1: INTRODUCTION

A granular medium is composed of particles which displace independently from one another and interact only at contact points [1]. The discrete character of the medium results in a complex behavior under conditions of loading and unloading [1]. To capture the behavior of a granular medium, a numerical method first developed by Cundall and Strack, called the discrete element method (DEM) is most widely used. The discrete representation has also been shown in the literature to effectively capture the degradation and failure by fracture of granular media such as concrete.

In this research work, the focus is on the application of DEM for uni-axial compressive behavior of a concrete cylinder. The behavior of concrete under uniaxial loading can be studied with three different approaches: Physical testing (experimental methods), analytical methods and numerical simulations. Experimental testing of this particular application is most reliable. As the dimensions of the selected sample are experimentally feasible, experimental results are much more reliable for the selected application. However, it is not always the best approach to go with, as there are several limitations to this, like experimental conditions. Analytical methods are also popular, but they are very tedious and not very efficient to use. These equations are derived from empirical correlations and are limited to their applicability. This approach is also used to validate and understand the results obtained from numerical simulations.

The third approach which is used in this research work is the use of numerical methods. Numerical methods are relatively easier to implement and flexible for testing compared to experimental testing. The results obtained by the simulations need to be validated with one of the two methods mentioned above. A Major advantage of

this method is that it has the capacity to test various input parameters with less time. This method allows the control over the parameters and allows control to predict the response of the model. This method also has an advantage that it allows to understand the variation of parameters which would be very time consuming and in some cases even difficult to understand through experimental procedures. It also has abilities to visualize and study the behavior of crack origination and propagation process within the model. Usually, this process is expensive in terms of cost and time to perform experimentally [2]. Numerical models are based on the continuum concept. Numerical models are representation of the material which can be continuous or discrete. Numerical modeling of unreinforced concrete can be done using finite element method as well as discrete element method. The choice of method in this work is the discrete element as it captures the movements and flows of the particles better than finite element methods.

Many finite element packages include nonlinear constitutive models for modeling concrete behavior. Although finite element is a popular approach to model mechanical behavior of concrete, the response of such a heterogeneous material is difficult to solve numerically due to the large displacements associated with it [3]. However, the discrete element approach is much more suitable for this kind of behavior since, it can capture more accurate behavior of the heterogeneous material and large displacements associated with it. DEM was first proposed by P.A. Cundall for studying large-scale movements in rock system [4] and was later developed for various particle models like bonded particle model [5], concrete particle model [6], jointed cohesive friction particle model, etc. This research work is based on the Jointed Cohesive Friction Particle Model (JCFPM) [6].

1.1 Thesis objectives

The objectives of the present study are:

- Develop a 3-dimensional DEM model for plain concrete cylinder under uni-axial

compression loading.

- To study and use the Jointed Cohesive Friction Particle Method(JCFPM) to initialize the interactions between discrete element particles.
- To study and analyze the influence of different input parameters of JCFPM method on the macro properties of the material.
- To calibrate the 3D model to the desired strength with the help of quantitative data from the parametric study.
- To validate the numerical stress-strain results with the known experimental results.
- Study the effect of poly-disperse particle generation method on the stress-strain response of concrete.

1.2 Organization of thesis

This thesis is divided into six chapters. Besides the introduction chapter, chapter 2 presents a general overview of DEM. The theory behind the contact model is explained in detail for both cohesive and non-cohesive type of interaction between discrete elements. Chapter 3 represents some more background about DEM and two contact models used in this research. Moreover, detailed mechanics behind jointed cohesive friction particle method model is discussed. Chapter 4 describes the implementation of the selected contact model in Yade open-source software. Particle generation, implementation of bonds and bond breakage criterion are discussed in detail. With Yade, particle generation module, packing density, distribution, effect of interaction radius is studied to optimize the particle size modeling parameters required for the modeling of DEM. It also involves the representation of the concrete cylinder and boundary conditions. Chapter 5 consists of the results of the numerical simulations. It also represents modeling parameter effects on the stress-strain response of the material. Parameters such as packing density, particle distribution inside the domain,

particle size, interaction range, cohesion and mono and polydisperse particle generation method are also discussed in this chapter. This chapter also discusses the bulk behavior of the material model. Chapter 6 summarizes all the results and important conclusions. The recommendations for future work are mentioned at the end of this chapter.

CHAPTER 2: LITERATURE REVIEW

The work performed in this thesis has two main objectives. First objective is to perform discrete element simulation to capture the response of uniaxial compression on the concrete cylinder and validate the model with the experiments performed in the laboratory. The second objective is to provide the input to a broader research program to understand the effects of different micro parameters. This work also validates selection of some of the micro parameters and their effect on the response of the material under uniaxial compression. This literature review is to provide the background information for this topic and basis for this research work.

This chapter is divided into two parts. The first part comprises of a review of discrete element modeling (DEM), and the second part is composed of the experimental and numerical studies done with respect to uniaxial compression test.

2.1 Discrete Element Modeling (DEM)

The discrete element modeling is a numerical technique in which mechanical response of granular materials/structures is studied effectively. DEM models can be used to study the fracture, large displacement, behavior location and to predict the macroscale response of various materials. Compared to the other continuum modeling methods, DEM is computationally more expensive and this particular requirement of DEM creates difficulties in industrial applications. However, with increase in computation power in recent times, DEM has become a choice of modeling in various industries such as mining, geotechnical engineering, civil engineering, powder metallurgy, food handling industry and automotive industry. This method is fast growing hand in hand with the boost in processing power and use of different algorithms to

perform nearest neighbor search. This allows to simulate large number of particles in the model using a single processor [1]. This increased ability allows DEM to perform simulations of structures consisting large number of particles like soils, grains, etc. First use of discrete element modeling started with the study of earth materials by Cundall & Strack [4] who explored the study of granular media with no cohesion. The study of soil with cohesion was done by Liu et al. [7]; examination of models of soil with cohesion was performed by Yao & Anandarajah [8] and also rock problems modeled with DEM are noted by Potyondy & Cundall [5] and Moon et al. [9].

DEM can be combined with other continuum software to model more complex and hybrid modeling as in case of earth-moving machines. One of such analysis involving soil-tool interaction, requires the hybrid finite-discrete element numerical modeling. This captures large displacement of soil particles and small deformation of the tool. Mechanics of material removal in rock cutting was studied by B. Aresh [10] using a hybrid finite-discrete commercial package. Along with this, in the modeling of rock cutting, consideration of the tool being rigid is discussed by J. Rojeck [11].

A numerical method must recognize the new contacts automatically upon every iteration and it must allow finite displacements and rotations of discrete elements in order to be considered as a DEM [4]. The numerical scheme will be limited to small numbers of bodies as the interactions are known in advance and no new contacts will be automatically detected. The second part is specifically important; otherwise, DEM will fail to produce the discontinuous medium.

There are two basic components of discrete element model, the elements and contacts between them. The elements are individual physical bodies mostly treated as rigid bodies or sometimes collection of individual bodies. The elements can have different shape, sizes and distribution over the domain. Considering computational cost, the circular particles or facets in 2D and spherical particles in 3D prove to give accurate model response and are easy to handle [12]. When the distance between

two elements is zero, they are said to be in contact but when this distance becomes negative, there is an overlap and magnitude of this overlap defines the compressive force acting on them. Other parameters like frictional force, normal and shear contact stiffness, damping coefficient, etc. are then calculated inside the contact model to model overall bulk behavior. In some contact models like the jointed cohesive friction particle model, contact normal and contact shear stiffness can also be mentioned manually and their ratio can be set to achieve the expected goal [6]; This serves as a major contributor and main contact model in this work. The contact model is described in detailed in section 3.3.

2.1.1 General model mechanism

Different particle models are available in DEM and those work with specific set of parameters proposed by Schneider et al. [13] and Potyondy and Cundall [5]. These particle models are used in various DEM packages available in the industry. However, there is a generalized mechanism behind every model which is briefly discussed in this section. There are mainly four different stages of the modeling which is used by many packages. They are,

- Particle generation and distribution
- Initiation of interactions
- Contact model
- Failure

2.1.1.1 Particle Generation And Distribution

The model volume is filled with the number of particles which represent the material properties under consideration. This basic process is termed as particle generation. Size of the particles is user defined. Many packages allow variable sized particles with different shapes and structures as mentioned earlier. For this thesis work, considering complexity of the simulation, particle shape is chosen to be spherical. The

spherical particles have brought interesting insights to the characterization of failure mechanisms in cohesive materials [6]. The aim is to model discrete elements which are in close proximity of the elements in the actual structure. In case of granular structures like concrete, sand or applications in mining, the geometry is filled with thousands of densely packed particles which need to be defined randomly. There are several particle generation algorithms in place. There are three main classes of these algorithms [12] which are described below.

1. Constructive algorithms:

Constructive algorithms are based on the geometry under consideration. Yade uses sweep and prune type of constructive algorithm [14]. This generates particles in a closed geometry. Once the particles are generated there is no need of any secondary arrangement or process on the particles. This makes the algorithm more efficient than other two algorithms. In this method, spheres of specific diameter defined by the user are placed at the axis aligned bounding boxes, which overlap only if overlap is along all the axes. The complexity of this algorithm is $O(n \log n)$. The algorithm makes sure that no newly created particles overlap with the previously created particle. If any such incident is occurred then the newly created particle is discarded from the model. This process is repeated until the domain is filled with the maximum number of tries to place a particle is reached and no new particle is accepted by the algorithm. As mentioned earlier, this method is only useful for the domain which is a closed structure. Figure 2.1(a) shows the domain filling process with the constructive algorithm.

2. Collective rearrangement algorithms:

In this particle generation algorithm, the user defines a fixed number of particles for the entire domain. The overall process takes place in two steps. In the first step, the defined number of particles are generated and are randomly placed in the domain. As the first step can have particle overlaps, in the second step, particles are

displaced as per their overlap magnitude. As this algorithm is two step, it is usually computationally more expensive than the constructive algorithm. Figure 2.1(b) shows the representation of the collective rearrangement technique.

3. Dynamic algorithm:

In this algorithm, the particles are initially located at random positions in a user defined plane, which can be called as particle generation factory and then are allowed to fall in the domain by gravity. For this particular algorithm, the domain of the required geometry is necessary in order to have rearrangement of the particles in the domain. This method is computationally most expensive as DEM solutions and particle generation happens at the same time. Figure 2.1(c) shows the particle generation from the top factory plane which are allowed to rearrange themselves in the domain simultaneously.

A size of the particle and total number of particles in the domain are fundamental phenomena for DEM modeling. Although it is difficult to represent each grain of the material with DE particle, it is important to have sufficient number of DE particles in the model to ensure high resolution to study the material behavior. The particle size distribution in case of spheres can be of 3 different types. Monodisperse [15], which uses single size of particles, Bidisperse [16], which uses two different sizes of particles in the domain and Polydisperse [17], which uses multiple sizes of particles for the particular domain.

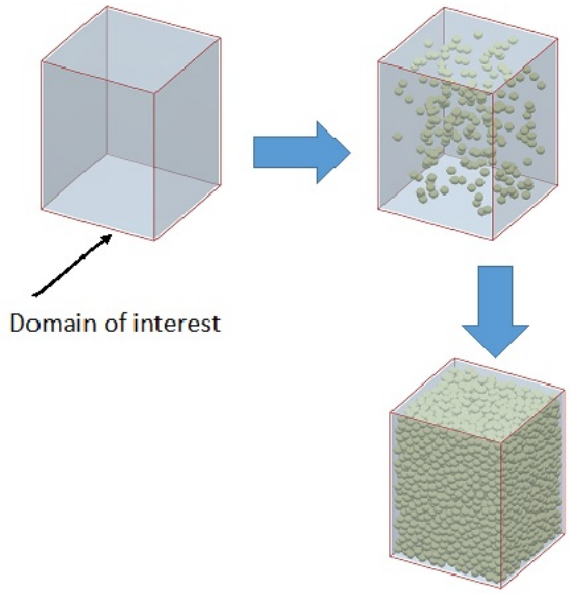

(a) Constructive algorithm

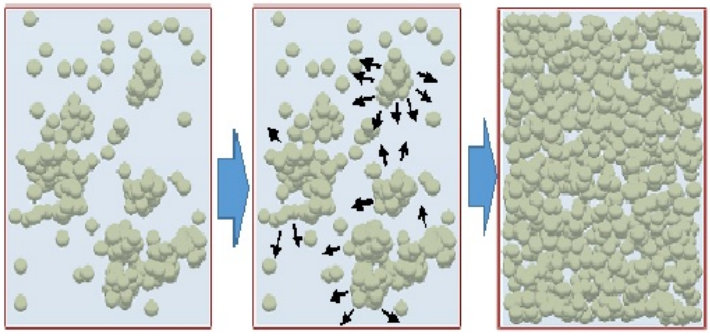

(b) Collective rearrangement technique

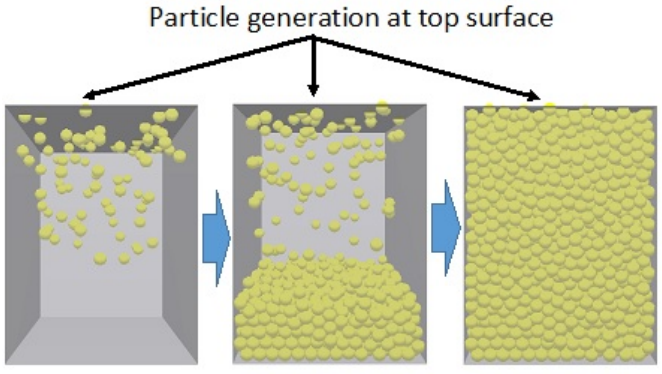

(c) Dynamic technique

Figure 2.1: Particle generation techniques in DEM [18].

2.1.1.2 Initialization of Interactions

Interactions differ between cohesive and non-cohesive materials in DEM. Inclusion of interactions as a cohesion is usually modeled in materials like cement where the joint between grains is found. These interactions are treated as bond between discrete elements in many models. There are various methods on the mechanism of these bonds like Bonded Particle Method defined by Potyondy and Cundall [5], Jointed Cohesive Friction Particle Model (JCFPM) [6], Concrete Particle Method (CPM) [14], etc. This research work mainly deals with JCFPM method for modeling. Unlike the classic description of the medium in many packages which allow interaction between only particles which are in direct contact, e.g. Itasca PFC [19], ESyS-Particle [6] and also the first version YADE [20], the current implementation of the model introduces a parameter called interaction range, which allows to link elements which are not in direct contact with each other but within the interaction zone. This parameter directly affects the interlocking between particles and has direct effect on the response of the material. Proposed work for this parameter also mentions about forming the numerical medium according to micro-structural complexity of the material model. Along with this, interaction range has direct effect on the coordination number and total number of bonds. The interaction range and its influence is discussed in detail in later chapters. These bonded contacts or interactions can then be treated accordingly to calculate relative resisting forces for the model. For any DE model, as the number of bonds go on decreasing, material starts to behave more granular in nature and the validity of the model needs to be verified [21].

2.1.2 Advantages of discrete element modeling

In DEM individual particles have their own velocity and forces. Each particle can influence other particle only when the two particles come in contact with each other. The shape of the discrete elements vary from application to application and

complexity. The basic technique uses spherical shaped particles whereas advanced techniques can have various shapes of particles. This is specifically important in case of the material which has arbitrary shaped composition. This composition can be modeled with very close accuracy with DEM. DEM is also capable of modeling heterogeneous material response better than FEM and is also capable of handling large displacements of particles, which is difficult to model with FEM. DEM allows to study the effects of various macro parameters of the material on the bulk response much more efficiently compared to FEM.

DEM is the choice of method in the applications where granular flows are especially important because, DEM has better flexibility to model the behavior of granular media as compared to other numerical techniques.
Following section describes some of the industrial applications of DEM and a few limitations for this modeling method.

2.1.3 Applications and limitations Of DEM

A method first proposed by Cundall and Strack in 1979 was first applied in the geomechanics. This method gives detailed insight into the mechanism of governing particle flow, contact behavior and detailed interactions at the particle level. DEM allows us to increase our knowledge regarding granular materials and help us to improve the design and operation of particulate systems. The complexity of the method finds its application in the modeling of natural processes like the landslide.

DEM finds its application even outside of the soil mechanics and geotechnical engineering. DEM has been widely used by chemical and process engineers, by food industry, mining engineering, geomechanical engineering, pharmaceutical science and automobile industry [22]. There are several DEM applications in process industry such as ball mills [23], silo filling [24], die filling for tableting [25], flow in screw conveyors [26] and granular mixing blenders.

As mentioned before, due to the computation complexity there are limitations in

the use of DEM for industrial applications. The important aspect of DEM models is the input parameters. Calibration of these input parameters in reasonable time is one of the difficulties with DEM. A DEM model is a simplification of real-life physical system. This consists of contact, deformation, geometry of the particles and number of the particles. However, as the real system usually has millions of particles with variable sizes and distributions, the calibration of input parameters essentially becomes time consuming.

To overcome this computation difficulty, O'Sullivan recommends use of 2D or 3D model numerical study. The advantage with 2D modeling is, it is computationally very cheap and is able to capture key mechanical response of granular particles. However, it comes with caution that it may be inappropriate to draw qualitative conclusions from 2D simulations as actual experiment is 3 dimensional and calibration of 2 dimensional model needs to be done with care.

2.2 Utilization of DEM in Geomechanics

DEM is commonly used in geomechanics simulations of both cohesionless and cemented sand/rock masses of bonded particles. Discrete element methods are usually applied to particles larger than 0.1 mm in size to ensure that the surface attraction forces are insignificant compared to the particle inertia [27].

As mentioned by O'Sullivan [22], DEM within geomechanics literature may be broadly classified into several categories as, DEM model validation and calibration, investigation of relationships between macroscale material response and microscale mechanics, modification of DEM algorithms, development of interpretation techniques, or simulation of field-scale boundary value problems.

Applications of DEM in the geomechanics are mentioned in the Fig 2.2. It is to be noted that there are far more studies than those listed in the Fig 2.2, however, to highlight the breadth of laboratory tests which have been simulated using DEM, only limited references are provided. The purpose of the list of studies is to show the

reach of laboratory element tests which have been studied using DEM.

Geomechanics Application	Reference
Uniaxial compression test	Wu et al. (2010)
Biaxial compression test	O'Sullivan et al. (2002)
Simple shear test	Matsushima et al. (2003)
Plane strain test	Powrie et al. (2005)
Direct simple shear stress	Dabeet (2014)
Triaxial compression test	Cui et al. (2007)
Brazilian test	Potyondy and Cundall (2004)

Figure 2.2: List of general application of DEM in geomechanics [22].

The use of DEM in the study of laboratory element tests is well established within the research community, with much of the focus on 3D simulations to accurately represent real-life conditions. Section 2.2.1 will provide a deeper look into the purpose of such studies, specifically parametric study of the input parameters of discrete element model and their effects on the behavior of the material.

2.2.1 DEM parameter sensitivity studies

One of the major advantages of DEM is the ability to perform parametric study of the model. The sensitivity of model behavior to specific material micro parameters can be studied effectively with DEM. Some of the important parameters include particle size, friction angle, number of particles, particle stiffness, and particle shape. This section provides an overview of past DEM studies utilizing laboratory element tests and DEM simulations to study the effect of model micro parameters on the material behavior.

A wide range of various laboratory tests have been performed to study the particle scale effects of the material behavior. Simulations of biaxial tests of steel rods[22]

consider the sensitivity of the model response to particle shape and surface friction. Wu et al. (2010)[24] performed uniaxial compression tests on asphalt to investigate the effect of variations in internal particle geometry, distribution of bond strengths and friction angle. Powrie et al. (2005)[11] used plane strain test on sand to test effects of porosity of the model and interparticle friction.

Studies mentioned in Fig 2.2 consists of steel spheres under triaxial loading to analyze the sensitivity of the macro-scale material response to the friction coefficient. Cui and O'Sullivan (2006) simulated direct shear box tests to investigate the effects of surface friction and particle generation approach.

Certain studies select ideal rod-shaped or spherical shaped particles to avoid numerical complexity and misinterpretation of irregular soil grains [22],[26]. However, many other researchers conducted studies on various shapes, which adds in the difficulty of accurately representing particle shape and distribution. Studies have also investigated the effect of particle size polydispersity, however very limited research has been conducted in polydisperse particle generation in the DEM[5].

It seems judicious, if one is not interested in investigating the effect of particle shape, one can go by selecting rod-shaped or spherical particles for the simulation to avoid complications in the model. By keeping the particle shape effect aside, more concentration can be given on the other micro parameters such as particle friction, size, stiffness, polydispersity and various boundary conditions.

2.2.2 DEM studies on the effect of particle size

Effect of particle size has been studied by very few researchers making it very difficult to find research work related to it. No DEM studies were found on the effect of particle size on the calibrated DEM. Even though there aren't many sources available, some notable studies related to the effect of particle size and angle of repose on the ultimate compressive strength of concrete under uniaxial compression load[18] is summarized in the following section.

The effect of particle size on the angle of repose has been studied experimentally with the monodisperse powders[13] and granular material in a rotatable drum apparatus[26]. The general conclusion drawn is that an increase in particle size will decrease the angle of repose. Cartensen and Chan(1976) suggested that the particle size effect in powders is related to particle cohesive force and sliding friction coefficient, particularly, coefficient of sliding friction decreases with increasing particle size.

Another research conducted by N. Tannu states the effect of particle size in the concrete medium on the ultimate compressive strength of concrete under uniaxial loading. The conclusion drawn is as the particle size decreases the packing density of the model increases. Furthermore, with the decrease in particle size, the ultimate compressive strength and strain to failure are increased. However, below a particular particle size, this effect is no longer significant. The conclusion that can be drawn from this study, is that, after a particular resolution of the model, further decrease in particle size would only result in increase in computation cost.

It can be seen from this attempt that, reviewing DEM studies on the effect of particle size is quiet rare within the research community. Some studies of cemented material are available, but more research on this parameter must be conducted. As concrete has various particle size distributions, it seems natural to conduct study on the effect of particle size on the material behavior. In this thesis, several micro parameters are studied; therefore, eliminating the variability of particle size in a given computer simulation is important.

2.2.3 DEM studies on effect of interaction range

The concept of interaction range is introduced by Scholteś et al. (2011) in his contact model called jointed cohesive friction particle model (JCFPM). This model behavior is different than traditional bonded particle model proposed by Cundall [5]. The traditional bonded particle model fails to reach the high ratio of compressive

strength to tensile strength, which results in over prediction of material strength[6]. Interaction range allows interaction between particles within the range which results into better interlocking between particles which enables JCFPM to overcome the above limitation. One of the objectives of this thesis is to study the effect of interaction range on the axial stress-strain response of the concrete material.

Scholteŝ et al. (2011) studied the effect of interaction range in his research and the conclusion drawn was that, as the interaction range is increased the ultimate compressive strength of the model increases. As the interaction range is increased, more number of links are formed in the model and particle interlocking is better, which results into the increase in the force required to break the bond between two particles. However, as claimed in the literature, brittleness of the model is increased with increasing interaction range.

It seems wise to understand and test the effect of interaction range in more detail as it directly affects the stress-strain response of the material. In this research, focus is given on understanding the effect of interaction range, however, as there are only few researches done regarding that, it is difficult to co-relate and decide the appropriate value for interaction range coefficient.

2.2.4 Calibration of DEM models using uniaxial compression test

One of the objectives of this thesis is to investigate the effects of various input parameters on stress-strain response of concrete under uniaxial compression loading. Previous studies indicate that uniaxial compression testing is particularly suited to calibrate and test the micro parameters of material in DEM simulations. This section focuses on summarizing past DEM calibration studies that have utilized uniaxial compression testing and explain the reasoning behind the selection of uniaxial compression as the laboratory test for this research.

In uniaxial compression test, axial stress is applied to the specimen and strains in any direction are not constrained. Shear and compressive stresses, axial and radial

strains can be observed during the test. However, it is difficult for a specimen to fail in shear, hence, compression is the primary source of strain[21].

Walsh (1998) simulated uniaxial compression tests to investigate the effects of initial specimen density on the stress-strain response of a granular medium under uniaxial compression. It is also mentioned in the research that the friction angle determined from the two dimensional soil models were lower than those found in three dimensional soil models. Several other studies which include the effect of particle rigidity, lateral earth pressure measurements and crack nature are deliberately not included since, they are beyond the scope of this research.

Chung and Ooi (2006) [28] studied particle friction parameters through three-particle sliding tests, and particle elastic modulus was calibrated by single particle compression tests. Furthermore, Chung and Ooi simulated uniaxial compression tests of corn grains and glass beads for comparison with laboratory results. Along with this, the process of load transmission was also studied by same authors.

This overview indicates that, a well designed uniaxial compression serves as a good test for providing inputs to the DEM researchers. Some applications include simulation of corn grains; even though not directly related to this research, it justifies the usefulness of uniaxial compression testing in model calibration. Based on the literature mentioned in this section and experimental testing performed by Pando and Flores [29], uniaxial compression of concrete was selected for this thesis.

2.2.5 DEM modeling of uniaxial compression response of concrete material

This section provides a general overview of existing numerical studies of concrete under unconfined compression test, particularly those with combined experimental and numerical methods. As there are only limited researches available which studies the effect of various DEM parameters on the response of the material, only the work related to the effect of packing density, particle size and interaction range is mentioned in this section.

Some studies in literature have combined laboratory tests with 3D DEM models [30]. It was shown that DEM is capable of modeling uniaxial compression of concrete cube specimen. Results of simulations performed were validated by the laboratory experiments and results of DEM simulations strongly correlated to the experimental results. Literature also mentions that the compressive strength, Young's modulus and stress-strain response can be reproduced with high accuracy [30].

Experiments performed by Walsh studied the local constitutive model for DEM and tested with uniaxial compression of concrete material. Conclusions of this study can be summarized as, the DEM model presents an accurate and reliable numerical method for uniaxial compression test of geomaterials and concrete under mechanical loading [31]. However, it is mentioned that, further validation is still needed to asses its convergence for the non-linear analysis of cohesive materials in terms of number and size of the discrete elements.

There are very few studies available on the effect of various DEM parameters on the stress strain response of the material. Scholtès (2011) [6] studied the effect of interaction range on the stress-strain response of the material. The conclusion drawn was, that, as the interaction range increases the ultimate compressive strength (UCS) for the respective material increases with small increase in peak strain value. However, only this literature talks about the effect of interaction range and hence this opens an area for young researchers to study this parameter further.

From the examples above, it is clear that numerical simulations are able to accurately model the uniaxial compression test on concrete material. Having experimental results for calibration and comparison increases the assurance of choice of the method. On the basis of this literature survey, the selected method for numerical analysis of concrete under compression is the correct choice of method. In this thesis work, uniaxial compression test is used considering two main factors; Firstly, the laboratory experiments performed by Pando and Flores [29] are available for calibration, and sec-

ondly for parametric study of the effect of particle size, packing density, interaction range, cohesion between particles and particle generation techniques.

The results of this thesis aim to supplement those from Scholtès et al. 2011, who first noticed the significance of interaction range on the stress strain behavior of material. By calibrating an equivalent DEM model with accurate uniaxial compression laboratory tests, this thesis aims to provide further insights into the effect of various other input parameters and to create a base for further research steps in the compression testing of concrete using DEM.

CHAPTER 3: BACKGROUND TO THE DISCRETE ELEMENT METHOD

This chapter provides basic knowledge about the discrete element method, its formulations, contact model and interaction mechanism. This chapter provides an overview of the basic concepts used in DEM to have better understanding of this research work.

3.1 Background

Basic principle behind the discrete element method is to divide the domain of interest into a collection of small and large number of discrete element particles. These particles are considered to be rigid in nature, and they behave like an individual body inside the domain. These particles contain the information about the micro properties of the material. These particles interact with each other at respective contact points and depending on the contact law for the particular model, forces and displacements are derived from them. The magnitude of the force on each particle is proportional to the magnitude of the overlap between two particles at contact. The interactions between the particles are divided into two different types, bonded and non-bonded. Depending upon the type of material, the interaction is defined. Cohesive material has bonded interaction whereas non-cohesive material does not need bonded interactions to get accurate response of the behavior. In case of the non-bonded model, a contact between the particles is necessary to get interaction forces on each particle. However, in case of the bonded model, a physical contact is not necessary between the particles. For the purpose of this research work, the chosen material is plain concrete, which is cohesive in nature. Hence, in the discrete element model, physical contact between particles is not necessarily required. The overlap

between the particles represents the particle deformation when they interact with each other. It is considered that the overlap area between the particles is comparatively smaller than the size of the particles. DEM works in several steps which include particle generation, collision detection, interaction creation, calculation of forces and displacement and numerical time integration. The flow chart of the overall DEM method is shown in Figure 3.1. According to the mechanism of DEM, as the contacts are determined, the forces resulting from particle interaction are determined using force-displacement laws depending on the type of contact model. With the help of Newton's second law, acceleration for each element is calculated. These accelerations are then time integrated to calculate the new positions of each element. The new positioned particles develop a new contact, and this process keeps on going until the end condition is specified as shown in Fig 3.1.

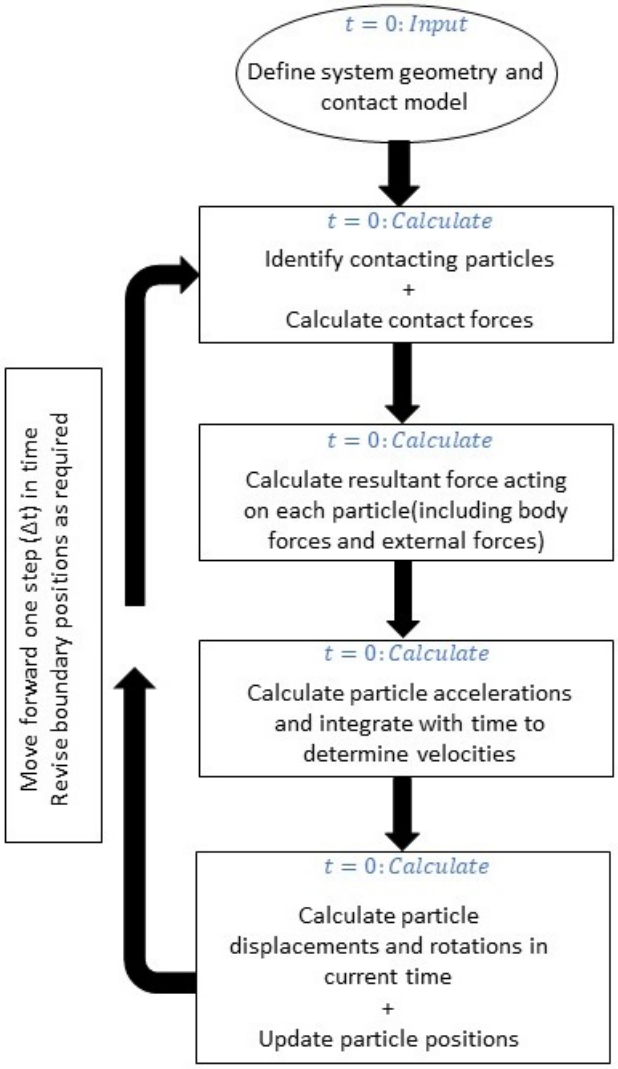

Figure 3.1: Generic DEM flow algorithm [22].

3.2 Contact Models

In this research work, suitable particle model for concrete structure is chosen to be cohesive particle model. Within the numerous cohesive models available in DEM, Jointed Cohesive Friction Particle Model(JCFPM) is chosen for this study. Particle models which are used to represent the behavior of the cohesive materials are required to have contact model that is capable of dealing with bonded as well as non-bonded contacts. As the bond is broken, particles may come in contact with each other and

to capture those interactions, a non-bonded contact must be available in the model. Numerical simulations in this research work are performed using an open source DEM package YADE (The Yade project) [14]. There are several particle models available in Yade and being an open source code, one can even modify the base script to include and modify the different particle models. The implemented contact model in the code is based on the recent research of Scholtès and Donzè [6]. The model is described in detail in the following sections.

3.2.1 Linear(Cundall) Contact Model

Linear contact model was first proposed by Cundall in 1979 [27] and is widely used in the discrete element method. Highlight of this model is, the normal force F_n is a linear function of normal displacement, which is the overlap between DE particles while the shear force is a linear function of shear displacement. However, shear force is limited by the Coulomb linear friction in the model. This model is implemented in Yade by Law2_ScGeom_FrictPhys_CundallStrack().

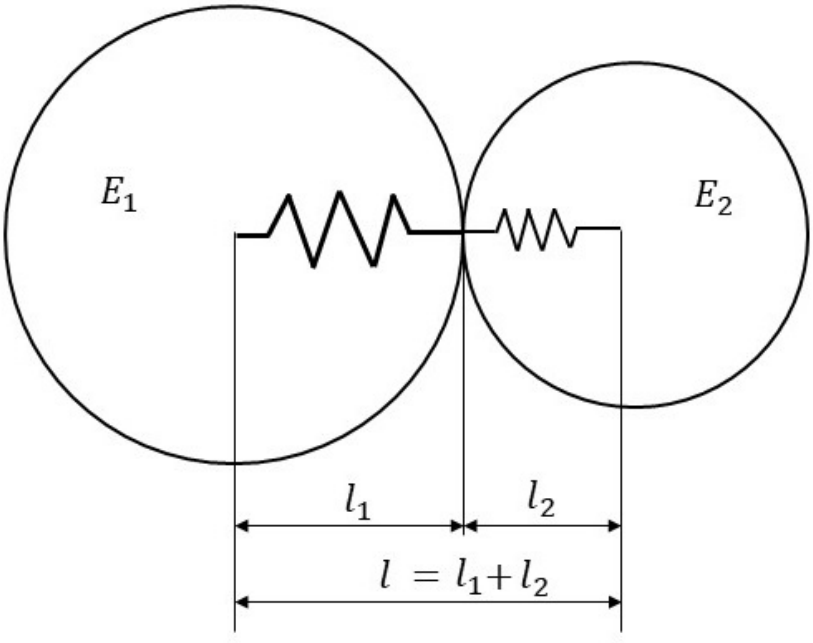

Figure 3.2: Representation of normal stiffness of contact between two contacting particles.

As shown in the Fig 3.2, the two particles are connected to each other by imaginary spring. These imaginary springs allows the necessary interaction between discrete element. Normal stiffness of the spring is related to Youngs̀ modulus of the both particle materials. To define the contact stiffness, the contact area between two particles needs to be defined correctly. Consider the two particles in the Fig 3.2; The total length of the spring is the addition of two individual spring lengths $l = l_1 + l_2$. Each spring has the length equal to the radius of individual particle l_i. The effective length between two particles is the total length minus the overlap. The contact area is defined as,

$$A = \pi min(l_1 l_2)^2 \tag{3.1}$$

The connector can be considered as an imaginary cylinder having the radius of the lesser sphere, spanning between their respective centers. Hence, the normal stiffness

of the spring is,

$$k_n = \left(\frac{l_1}{E_1 A} + \frac{l_2}{E_2 A}\right)^{-1} \tag{3.2}$$

Where, E_1 & E_2 are the respective Youngs̀ modulus of each particle. The tangent stiffness is a fraction of k_n, given as,

$$k_t = \left(\frac{k_t}{k_n}\right) k_n \tag{3.3}$$

where the ratio is the average between two materials in contact.

Friction angle on the contact is computed as following,

$$tan\phi = min[(tan\phi)_1, (tan\phi)_2] \tag{3.4}$$

However, the material without friction will not have frictional contacts, regardless of friction of the other material.

The normal force response is computed from the normal displacement,

$$F_n = u_n k_n \tag{3.5}$$

and the contact is broken when $u_n > 0$.

The tangential force is incrementally computed from tangential relative velocity $\dot{u}$ and may get reduced to coulomb criterion.

$$\Delta F_t = (\dot{u})_t \Delta t k_t F_t^T = F_t + \Delta F_t \tag{3.6}$$

The Elastic potential stored in a contact is the triangular area below the force-displacement diagram and is given by,

$$\frac{1}{2}\left(\frac{F_n^2}{k_n} + \frac{F_t^2}{k_t}\right) \tag{3.7}$$

Plastically dissipated energy is the elastic energy removed by the tangent slip, which is an area ABCD as shown in Fig3.3.

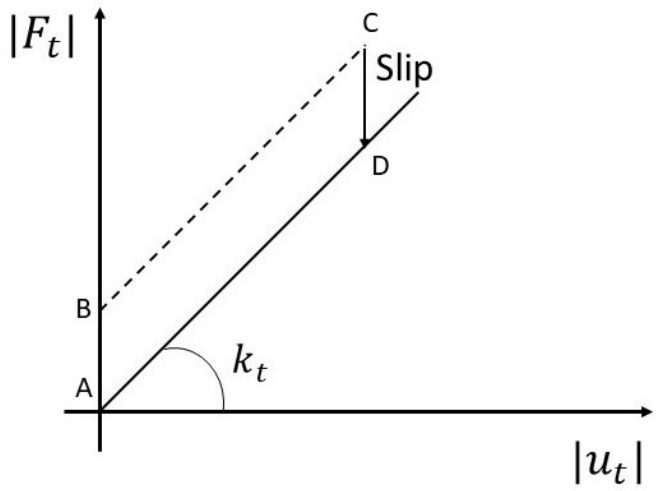

Figure 3.3: Linear contact model for energy dissipation in slip.

3.2.2 Jointed Cohesive Friction Particle Model

The mechanical behavior of cementitious material is modelled in DEM using inclusion of bonds between discrete elements. There are various methods and models to govern the behavior of these bonds like Bonded Particle Model, concrete particle model, etc. The ratio between uni-axial compressive strength (σ_c) and the tensile strength (σ_t) of brittle rocks is one of the most important characteristics of any model [32]. Even though the compressive response is the most widely used parameter to characterize the rock, the ratio mentioned above holds a good influence in the brittle failure of the rock. The study of DEM has brought deeper knowledge to the characterization of failure mechanisms in cohesive materials. However, there are some limitations to the basic formulation of models. These various models are not able to reach high (σ_c/σ_t) ratio which is a representative of brittle rocks [5][31]. One drawback of this is, while calibrating compressive strength of the material, it results in the over prediction of its related tensile strength. This can be the point of problem where the nature of the stress maybe tension or compression [6].

This limitation of classical DEM models can be overcome by an additional texture

property like irregular shape or improving the grain interlocking. Thus, a model which is capable of accurately replicating the material behavior must have the flexibility to include these texture properties. The limitations with the irregular shaped particles include the computation complexity and cost. Another approach includes enhancing the micro-structure of the packing by increasing the bond density between the particles. This approach was proposed by Donze et al.(1997) [33]. However, no precise analyses have been performed to validate the approach, considering the macroscopic response of the simulated medium.

The modeling method proposed by Scholtes and Donze in 2011 called as the Jointed Cohesive Friction Particle Model overcomes the limitation in classical modeling methods. This model represents a formulation capable of properly simulating the microscopic behavior of material. The formulation provides the balance between the accuracy of the response and computation cost. Use of spherical particles with this approach is best suited to replicate the material response with considerable accuracy. The advantage of this method is that, the higher values of (σ_c/σ_t) ratio can be obtained and can be manipulated as well. This method introduces a parameter which controls the grain interlocking between the discrete elements. By adjusting the value of the interlocking, the macroscopic response of the material can be simulated to the targeted material behavior. The brief description of the JCFPM model is mentioned below.

As shown in the Fig 3.4, the interaction force F represents the action of particle A on particle B, which is composed of normal force F_n and a shear force F_s. These forces are related to the relative normal displacement and incremental shear displacement through normal stiffness k_n and shear stiffness k_s at the contact area.

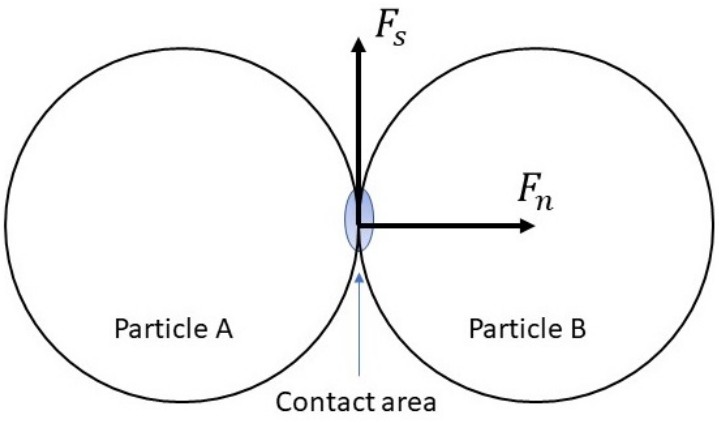

Figure 3.4: Representation of normal and shear force between two discrete elements.

The calculation of normal interaction forces is performed through local constitutive law as shown in Fig 3.5. It can be split into two components, compressive and the tensile component. In compression, F_n is linear and is given by,

$$F_n = k_n \Delta D \tag{3.8}$$

where, F_n is the normal force, ΔD is the relative displacement between the interacting discrete elements, and k_n is the normal stiffness given by,

$$k_n = E_e q \frac{R_A R_B}{(R_A + R_B)} \tag{3.9}$$

where, $E_e q$ is an equivalent bulk modulus and R_A & R_B are the respective radii of the discrete elements.

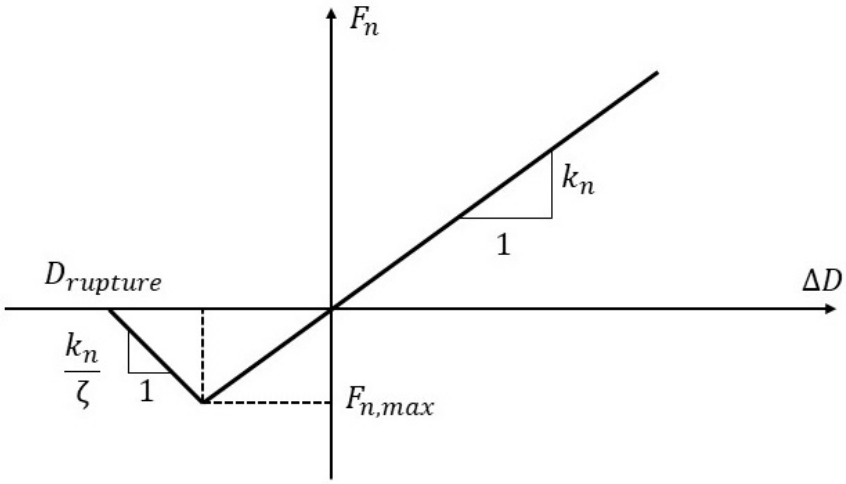

Figure 3.5: Constitutive law for normal interaction force [6].

In tension, the maximum acceptable tensile force $F_{n,max}$ defined as a function of tensile strength t is given as,

$$F_{n,max} = -tA_{int} \tag{3.10}$$

where, $A_{int} = \pi(_{min}(R_A, R_B))^2$ is the contact area between particles [6]. After maximum tensile force is reached, the stiffness can be modified by a term called softening factor ζ to control the energy dissipation due to breakage as,

$$F_n = (\Delta D - D_{rupture})\frac{k_n}{\zeta} \tag{3.11}$$

When, $\Delta D > D_{rupture}$ tensile rupture takes place and forces are reset to zero. However, in the current version of Yade DEM package, which is used for the simulation in this research work, the value of the softening factor ζ is non-adjustable and is by default set to 1 [14].

The shear force F_s is computed in an incremental manner by updating its intensity and orientation depending on the increment of the shear force $\Delta F_s = k_s \Delta u_s$ which is developed at interaction point, defined by Hart et al. [34].

$$F_s = \{F_s\}_{updated} + k_s \Delta u_s \tag{3.12}$$

with k_s be the shear stiffness and Δu_s be the incremental tangential displacement.

A modified Coulomb law as shown in Fig 3.6 is used to model the non-linear behavior of the material. The maximum allowable shear force is given by,

$$F_{s,max} = F_n tan\phi_b + cA_{int} \tag{3.13}$$

where, ϕ_b is the local friction angle and c is the cohesion between discrete elements.

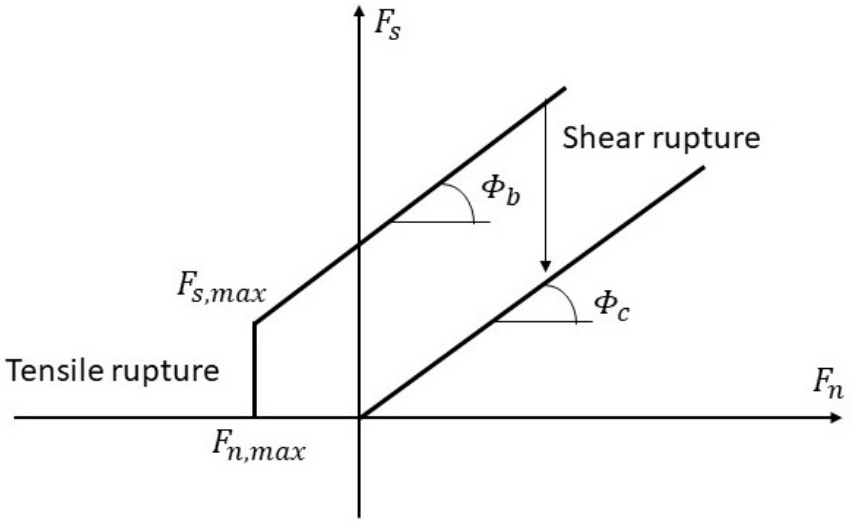

Figure 3.6: Modified mohr coulomb law. (Adapted from [6]).

Shear rupture occurs when $F_s \geq F_{s,max}$. After that, the interaction becomes purely frictional between discrete elements and the maximum shear force becomes,

$$F_{s,max} = F_n tan\phi_c \tag{3.14}$$

where, ϕ_c is the residual friction angle. In the current version of Yade,

$$\phi_b = \phi_c = \phi \tag{3.15}$$

is taken for the numerical calculations.

With the base developed in this chapter about JCFPM method, it is important to carefully model the setup of the numerical simulation with Yade. Yade is an open source software and has very limited user interface. The complete model, right from building its geometry, the boundary conditions, and loading it to obtain the required

output data is completely hand coded in python script by the user. This script is then compiled with Yade to get the required simulation output data. The next chapter talks about the modeling with yade in detail.

CHAPTER 4: DEM MODEL OF UNIAXIAL COMPRESSION OF CONCRETE CYLINDER

The interaction between discrete elements is due to the contact forces between them. The behavior and the response of the material is governed by these interactions. There are several different contact laws currently present in DEM which define these interactions. The selection of a contact law which would represent the behavior most accurately is very crucial and important in DEM. Yade has the capability to include various different contact laws. Yade is a general public license software framework, designed with dynamic libraries. This allows the user to add and modify the numerical models and their respective behavior for their own applications. The open source nature of the software provides a good flexibility and applicability for the research on the present material models. For the study of the cementitious material JCFPM method which is the method selected for this research uses two contact models, as stated in section 3.2.

As mentioned in section 2.1.1, there are different particle generation techniques in DEM. Each packing technique generates different particle arrangement in the domain. As mentioned in section 2.1.1, yade uses constructive algorithm for particle generation. Yade also provides different sub-packing arrangements like, random dense packing, hexagonal packing, orthogonal packing, etc. Different sub-packings generate particles in different orientation and are used for particular type of application. In the current research, the code is tested with two different packing methods, random dense and hexagonal packing to understand the effects and structure. Later random dense packing arrangement is used for this study. A brief description is given in the following section. The effect of packing arrangement, number of particles and packing density is mentioned in the following section.

4.1 Particle Generation And Packing In Yade

Particle arrangement inside the domain plays a crucial role in the response of the material in DEM simulations. The overall behavior in many aspects vary as per the packing. The chosen algorithm should ideally have the maximum possible dense structure of discrete elements in the domain. Due to the wide range of the particle sizes in the physical material like concrete, it is usually difficult to model every particle in the computer software. Some basic and plausible assumptions are made while developing the model to record the response of the material. Due to the time complexity and the cost of the simulation, simplest but accurate particle generation technique is used in Yade. As the particle arrangement inside the domain affects the macroscopic behavior of the material, the suitable method needs to be studied and taken into account while modeling for a respective application.

Different simulations are carried out to study the packing density of two different sub-packing algorithms. For the purpose of this study, hexagonal packing method and random dense packing method are studied. Out of these two methods, random dense packing method is chosen as it represents the true random nature of grain arrangement inside concrete. Also, packing density with different particle sizes and packing density with mono-disperse and poly-disperse distribution is also studied. Packing density is calculated as follows,

$$Packing\ density = \frac{total\ volume\ occupied\ by\ particles}{volume\ of\ the\ selected\ domain} \times 100 \tag{4.1}$$

where,

$$Total\ volume\ occupied\ by\ particles = volume\ of\ single\ particle\ \times\ N \tag{4.2}$$

where, N = total number of particles in the domain.

Selected dimension and parameters for the mono disperse and poly disperse distribution are discussed in the following section. Particle size is varied from 0.25 mm to 1.25 mm to study the packing density of mono disperse distribution. Table 4.1 provides the domain information and table 2 gives information about packing densities

according to the particle size.

Table 4.1: Dimensions of the test sample selected for this research work

Height of cylinder (mm)	Diameter of cylinder (mm)	Total volume $(mm)^3$
100	50	196349.57

Table 4.2: Calculated packing densities for different particle sizes of monodisperse arrangement.

Particle size(mm)	Volume of each particle $(mm)^3$	Total number of particles	Total volume occupied by particles $(mm)^3$	Packing density (%)
1.25	8.1812	11569	94648.3028	48
1	4.1887	23112	96809.2344	49.2
0.75	1.7671	56332	99544.27	50
0.5	0.5235	194857	102007	52
0.25	0.065	1604774	104310	53.5

The following Fig 4.1 shows the relation between size of the discrete element particle and the packing density. As mentioned above, particle sizes are varied from 0.25 mm to 1.25 mm radius of particle. The analysis observation shows that there is a linear relationship between particle size and packing density. It can be observed that as particle size goes on decreasing, the packing density of the particles goes on increasing. The maximum density obtained with the random distribution in Yade is observed to be 53.5% for 0.25 mm radius particle. Any decrease in the particle radius after this does not have a significant effect on the packing density. However, any change in the

radius of the particle changes the total number of particles by a very large amount.

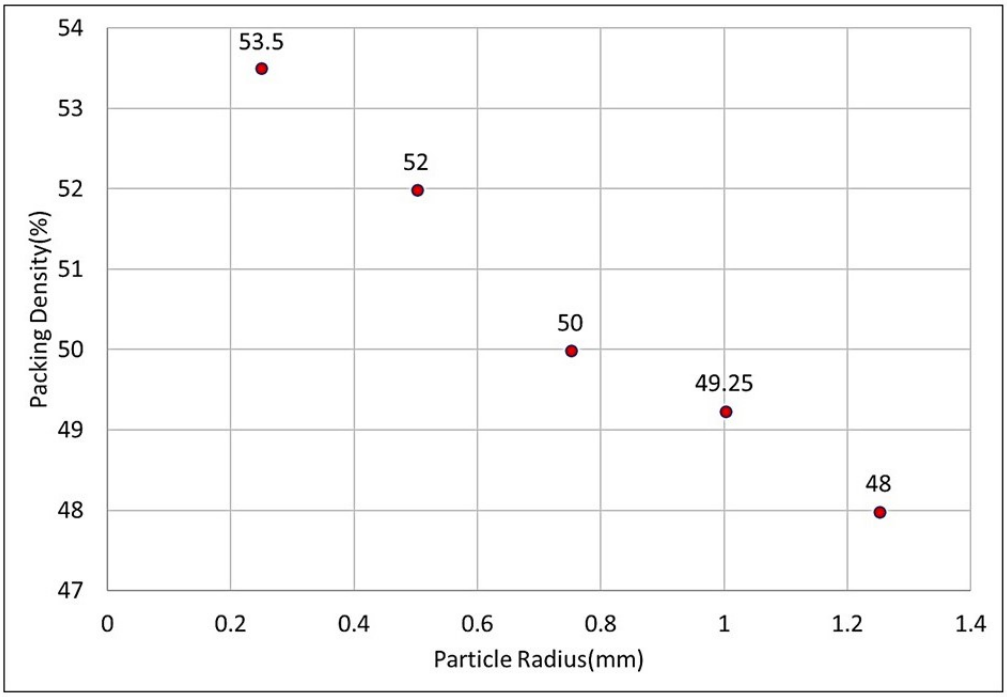

Figure 4.1: Effect of particle size on packing density.

For the purpose of this research, simulations with particles sizes 0.75 mm, 1 mm and 1.25 mm are chosen as they are relatively suitable for accuracy with less computation cost.

4.2 Bond Initialization

Bond models applied to simulate the behavior of cohesive material are different than other bond models as these models capture the joints between concrete grains to the desired accuracy. In the current research work, these bonds are represented by JCFPM which is capable of resisting the separation of the particles as well as governing the mechanism of non-bonded particles. An initial criterion must be defined to determine which particles are bonded to each other. This criterion exists in the JCFPM which must be met by particles to be considered as bonded. A user defined range called Interaction range is used for the bonding in this method. Particles

coming under this range are considered bonded. This provides the flexibility for grain interlocking inside the material. Interaction range is defined as follows,

$$Interaction\ range = R_i + (\gamma R_i) \tag{4.3}$$

where, R_i is the radius of the respective particle and γ is the interaction range coefficient. Table 4.3 represents the parameters used for the bond formation between discrete elements.

Table 4.3: Bond parameters used for bond formation.

Young modulus	Poisson's ratio	Bond stiffness	Interaction radius	Cohesion
E	ν	k_n, k_s	γ	t

The parameter γ defines the interaction range coefficient, which helps search for a contact with the neighboring particles which are not directly in contact with each other. Thus any two particles which are not directly in contact with each other can still be bonded together. This allows user to control the grain interlocking which then affects the behavior of the material. If the interaction range coefficient is increased, the number of bonds increases. If this parameter is set to be 1 then the bonds will be created within the particles which are in direct contact with each other and hence this model can be transformed in the other known models in DEM. The following Fig 4.2 represents the effect of interaction range.

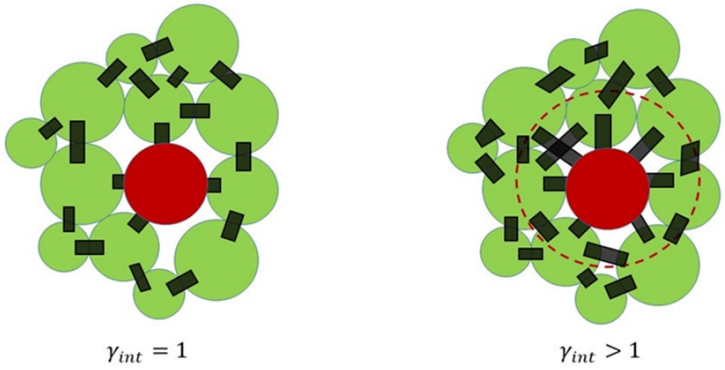

Figure 4.2: Graphical representation of interaction range.

4.3 Failure Criteria

For cohesive material like concrete, the material will have a microscopic failure when compression induced tensile loading on two cemented elements exceeds the bond strength. The material will undergo total failure when enough number of bonds are broken. The property of bond breakage between particles when bond strength exceeds at any point inside the domain gives an advantage over FEM in terms of crack origination and propagation.

Failure of bonds in the DEM requires a criterion through which bonds between particles can break. This mode is predefined in the material model used for the modeling. For the JCFPM model discussed in section 3.2.2, this criteria is based on the limits of the forces given in the same section.

4.4 Modeling

This section defines the modeling of the test specimen with DEM in Yade. Guided by the material and behavioral properties of concrete, a set of parameters is decided to guide the modeling of the test specimen. The predictive capabilities of the calibrated

parameters are simulated using a cylinder of the dimensions mentioned in section 4.4.1, which are exactly same as used in the experimental tests[29]. For the loading configuration and the geometry, the effort is to get the material response as close as the physical experimental tests under uniaxial compression performed by Pando and Flores [29]. The cylinder geometry, material properties and contact properties are discussed in the following.

All simulations were carried out by Yade, an open source DEM code. Simulations were performed on a local Ubuntu system at UNC Charlotte with 16 GB RAM.

4.4.1 Geometry

Fig 4.3 shows the test cylinder geometry and the DEM model. Yade requires an initial domain volume for the generation of particles. As discussed in chapter 1, constructive algorithm is used and spherical shaped particles are coded in the python script. The particle sizes and distribution are manually inserted in the packing module function included in the python script. Once the particles are generated and contacts are established, the respective position of particles is stored in the simulator. To simulate the uniaxial compression behavior of the material, a condition is given, in which two sets of bodies located around each end of the cylinder are allowed to displace towards each other. This is similar to the approach of having two invisible plates at both ends and are displaced towards each other as shown in Fig 4.4

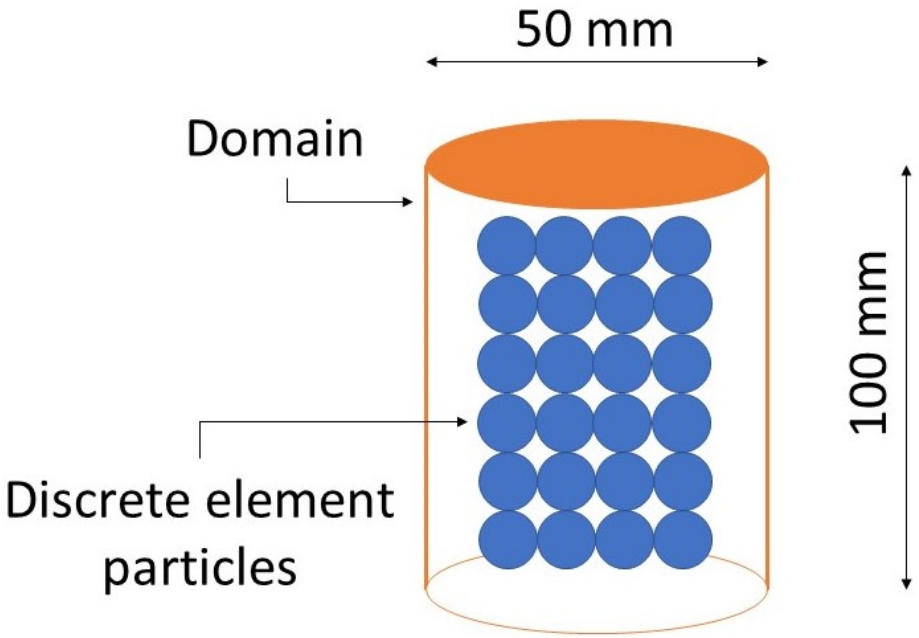

Figure 4.3: Graphical representation of the domain.

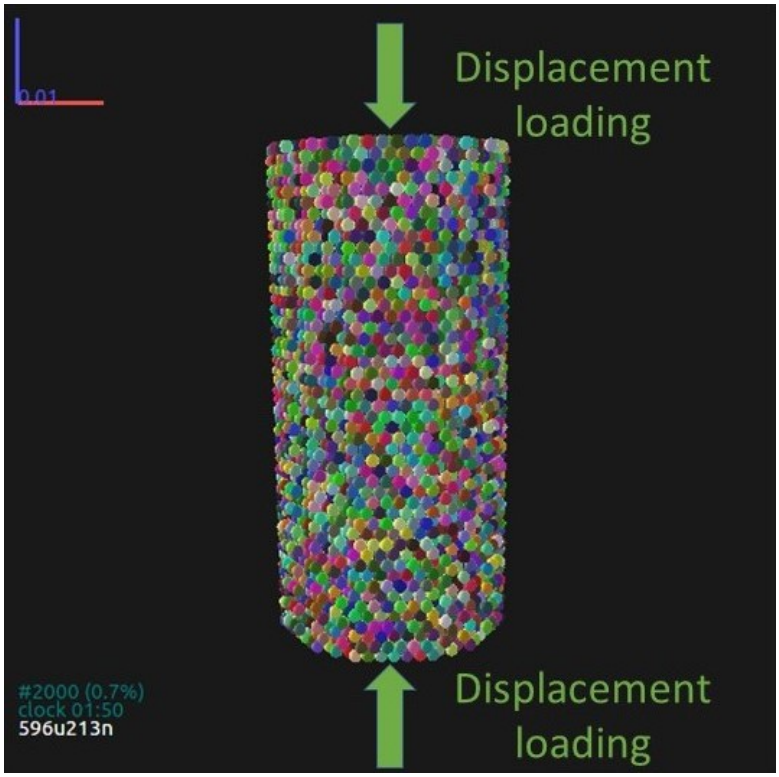

Figure 4.4: Graphical representation of the test sample.

4.4.2 Boundary Conditions

The loading configuration for uni-axial loading in the current model is achieved through displacement loading at the top and bottom ends of the cylinder. In this particular code, this is achieved by an inbuilt function in Yade which allows a group of bodies perpendicular to the loading plane on respective end of the cylinder to move towards each other with particular velocity along the loading axis, z-axis in this case. To maintain the quasi-static loading, the loading rate should be small enough compared to the size of numerical problem. To have this condition maintained in the current study, loading rate is set to be $0.05mm/ms$. As DEM simulations are fully dynamic, a local non-viscous damping is necessary in the model to dissipate kinetic energy [5]. The simulations in this code are run with the numerical damping of 0.4 [6].

4.4.3 Model Parameters

The DEM is very much parameter sensitive numerical method. Every parameter, right from the type of the particle to its material properties, has its own impact on the response of the material. In this study, according to the application, the rigid discrete element particles are selected for modeling. A set of parameters were decided that were capable of predicting the behavior of concrete material. These parameters were used to create simulations to predict the bulk behavior of concrete.

The material parameters for the simulation are given in Table 4.4. The values for the simulation are taken from the laboratory experiment and general material properties of concrete. Even though in the further study, the value of cohesion is changed to understand the direct effect on the material response, value mentioned in the table provides with the best material response for a particular particle size. Details about the parameter are discussed in chapter 5.

Table 4.4: Bond parameters used for current DEM model.

Parameter	Description	Value
ρ	Density (kg/m^3)	2400
E	Young's Modulus (GPa)	17
ν	Poisson's ratio	0.15
σ_t	Tensile strength (MPa)	3.163
c	Cohesion (MPa)	9
ϕ_c	Friction angle (Deg)	34.25
γ	Interaction range coefficient	1.4

Parameter values for bond stiffness between two particles are calculated internally as,

$$k_n = \frac{2E_1R_1E_2R_2}{E_1R_1 + E_2R_2} \tag{4.4}$$

$$k_s = \frac{2E_1R_1\nu_1E_2R_2\nu_2}{E_1R_1\nu_1 + E_2R_2\nu_2} \tag{4.5}$$

Thus, stiffness parameters change as per the particle radius, which makes the model less affected by the size of the particles in model as proposed in literature [6]. However, this claim is tested in the further research and described in chapter 5. Table 4.5 shows the calibrated bond parameter with varying particle size. As seen in the Table 4.5, the ratio of k_n/k_s is 6.66 in all the cases except with the particle size of $0.25mm$ radius.

Table 4.5: Calibrated bond parameters for various particle sizes.

Particle size (mm)	E(GPa)	ν	γ	Packing (%)	k_n	k_s
0.25	17	0.15	1.45	53.5	4.25	0.63
0.5	(17	0.15	1.45	52	8.5	1.275
0.75	17	0.15	1.45	50	12.75	1.9125
1	17	0.15	1.45	49.2	17	2.55
1.25	17	0.15	1.45	48	21.25	3.1875

CHAPTER 5: RESULTS AND DISCUSSION

In this chapter, the response of a concrete cylinder under the action of uni-axial compressive load is studied. A parametric study is carried out to analyze the effects of various input parameters on the response of the concrete cylinder. The bulk mechanical properties such as strain at failure and ultimate compressive strength for each parameter variation are evaluated and compared. The values of particle size, packing method(mono-disperse and poly-disperse), interaction range, cohesion, particle distribution(random and hexagonal), and packing density used and compared to obtain the required material response are discussed in the following section.

5.1 Stress-Strain Response Of Concrete Cylinder

Uni-axial compression test is the most widely used method to determine the compressive strength of a material and hence is used in this research. It is also known as the prime engineering property in case of concrete material. A schematic of the displacement controlled uni-axial compression is shown in Fig 5.1. If the graph of nominal stress versus nominal strain is plotted, the maximum stress reached is called as ultimate compressive strength (UCS) and the strain corresponding to UCS is called the strain at failure. In this study, to obtain accurate results with less computation time, a particle size of 1.25 mm radius is chosen to calibrate the DEM model to the experimental results provided by Pando and Flores[29]. The axial stress-strain curve obtained is shown in Fig 5.2. Later in the study, the effect of particle size variation is discussed in detail.

Average stress (σ_{avg}) and average strain (ϵ_{avg}) are calculated for model comparison are as follows,

$$\sigma_{avg} = \frac{(\sum Positive\ forces) + (\sum Negative\ forces)}{2 \times (A_{c/s})} \tag{5.1}$$

where, $Positive forces$ & $Negative forces$ are the forces at two ends of the cylinder and $A_{c/s}$ is the cross section area at two surfaces of the cylinder normal to the loading axis.

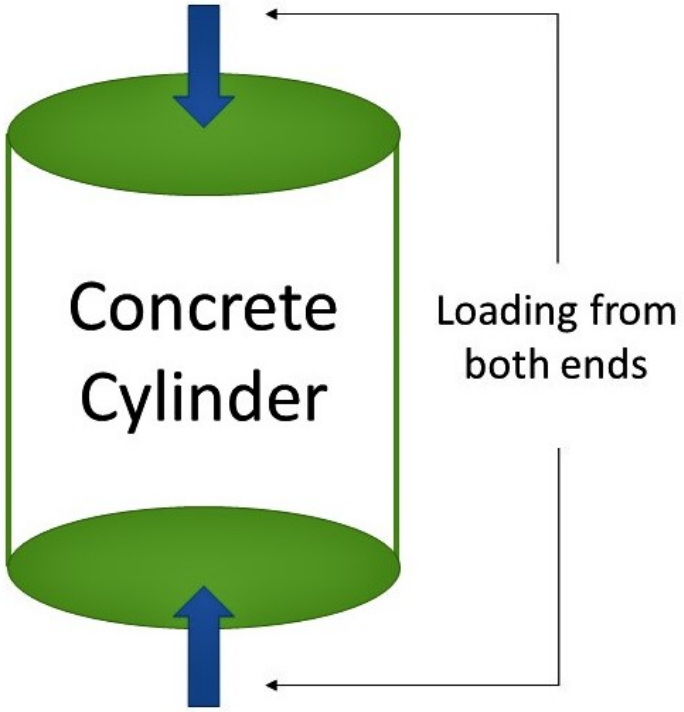

Figure 5.1: Graphical representation of the uni-axial test.

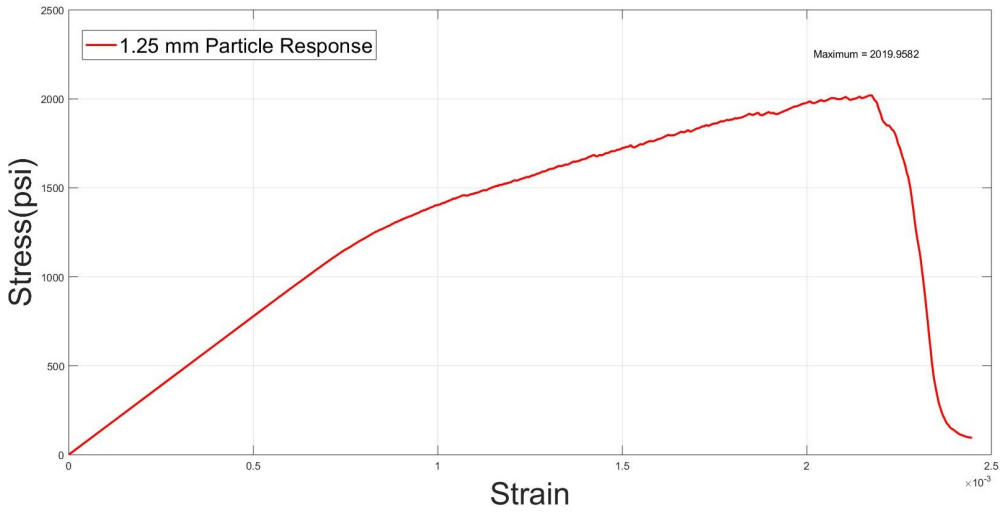

Figure 5.2: Predicted stress-strain curve for monodisperse particles of 1.25 mm.

The average strain is calculated as,

$$\epsilon_{avg} = \frac{Current\ height\ of\ cylinder - Initial\ height\ of\ cylinder}{Initial\ height\ of\ cylinder} \tag{5.2}$$

Pando and Flores conducted an experiment[29] which is used in this study to calibrate the simulation results. The results obtained by the experiment are in psi and are shown in the Fig 5.3. For the purpose of this study, only the axial stress and axial strain of the first test sample is considered to calibrate the DEM model. As seen in the Fig 5.3, ultimate compressive strength for plain concrete is, 1990 *psi* which is approximately equal to 13.8 MPa and strain at failure is, 0.00197. The results obtained from the simulation for 1.25 mm particle size are listed in the table. The UCS obtained from the simulation is in MPa and equal to 14.0275 MPa. It is then converted to *psi* and compared with the experimental results. The UCS value from the simulation is 2019 *psi* which is within the 1.6% of the experimental value and strain to failure is 0.0022 which is within 10% of the experimental value.

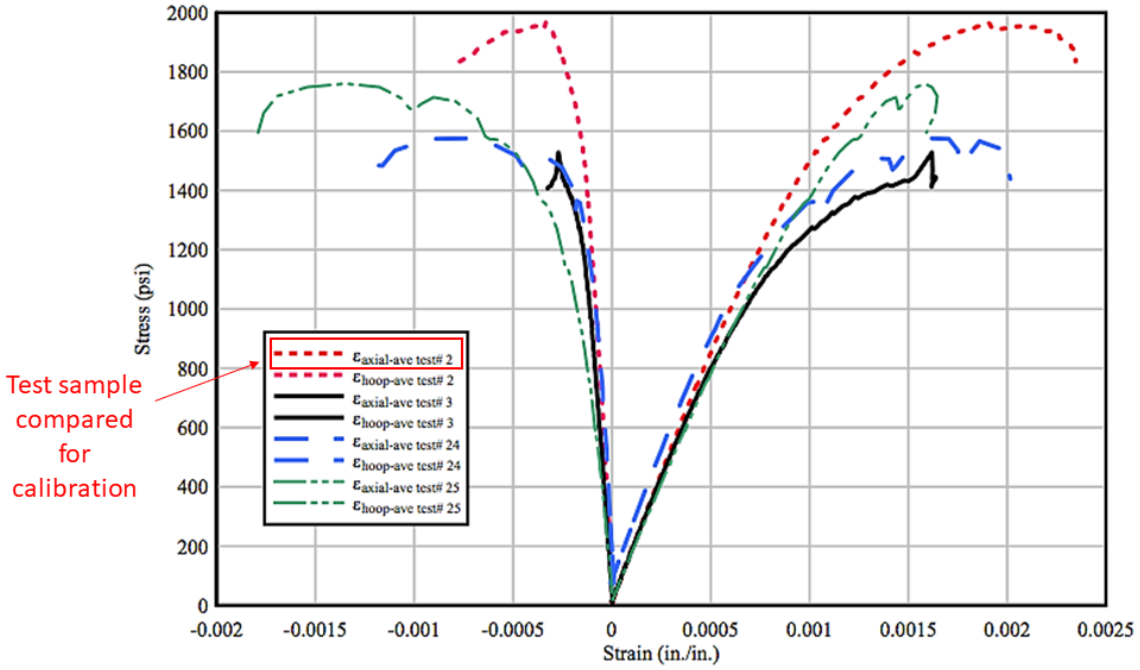

Figure 5.3: Experimental results for uniaxial compression test.

Table 5.1: Bulk material properties of material with particle size 1.25 mm.

Parameter	Description	DEM simulation results	Experimental results
σ_u	Ultimate Compressive Strength (psi)	2019	1990
ϵ_c	Strain to failure	0.0022	0.0021

The nature of the graph obtained from the DEM simulation represents two different slopes and change starts to occur at 0.001 strain. However, this change in the slope occurs approximately at 0.0015 strain in the experimental results. This indicates the deviation of numerical results from the experimental tests. The slope changing pattern of DEM curves is also seen in some of the literature at the point of material failure; However, no literature mentions about this behavior. To understand the cause behind this change, further studies on the calculation of stress and strain in the numerical code needs to be performed.

5.2 Effect Of Particle Size

To understand the effect of particle size on the response of the material in the DEM, three other particle sizes were considered in this study. Particle sizes, 0.5 mm, 0.75 mm & 1.0 mm were chosen as these particle sizes exhibit denser packing compared to 1.25 mm radius particle.

Keeping all the other parameters same, only the radius of the particles is varied to evaluate the three cases. Similar to 1.25 mm particle, stress-strain curve is obtained for different particle sizes. The effect of the particle sizes on the response of the material can be seen in the Fig 5.4. From the obtained results, it is observed that, the response of the material changes with the particle sizes. This contradicts the statement in JCFPM model, that particle sizes have no reasonable effect on the behavior of the material [6]. As particle size decreases from 1.25 mm to 0.5 mm, the ultimate compressive strength(UCS) increases from 14.02 MPa to 15.8 MPa. However, strain to failure does not get affected much. Strain to failure for 1.25 mm, 0.75 mm and 0.5 mm is observed to be 0.0022 and strain to failure for 1.0 mm particle is observed to be 0.0023.

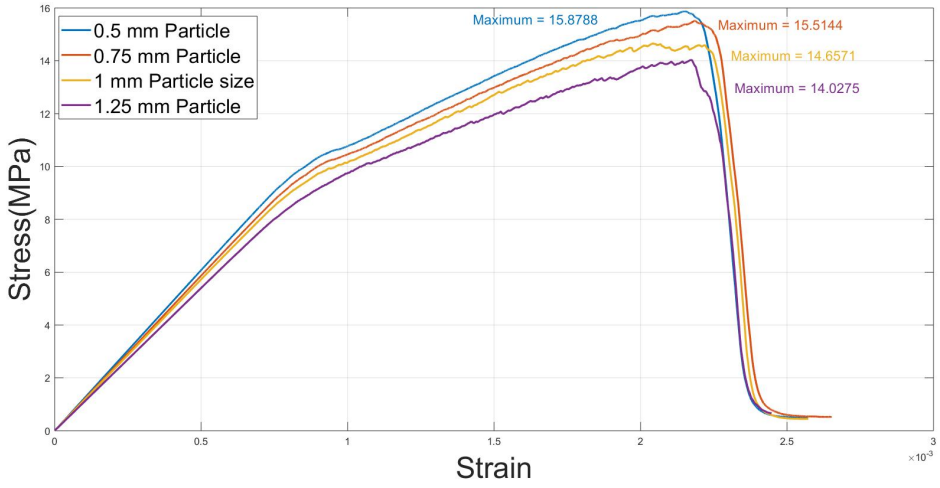

Figure 5.4: Effect of particle size on the stress-strain curve.

Even though the domain size and particle generation method is same for all the

cases, the number of particles inside the domain varies with the size of particle. This increases the packing density of the overall domain as shown in Table 4.5 and can be seen in the following Fig 5.5. Also, the position of each particle for each simulation is random inside the domain.

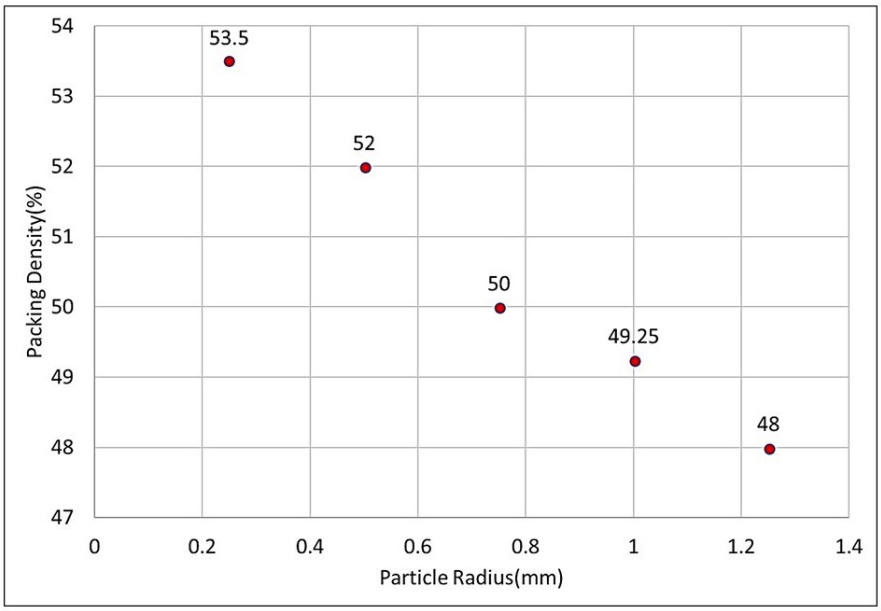

Figure 5.5: Effect particle size on the packing density.

Higher packing density leads to higher number of bonds inside the domain. Thus, the interlocking between particles is stronger than the domain with lesser packing density. Thus, higher force is required to break the bonds between elements, which might have lead to the increase in the UCS of the material. However, as we further decrease the particle size, the effect on the material stress-strain response is minimal. Therefore, it is safe to state that, after a certain resolution of the model, further decresae in particle size does not affect the material response.

The effect of particle size on the ultimate tensile strength and peak strain is shown in Fig 5.6 & Fig 5.7 respectively.

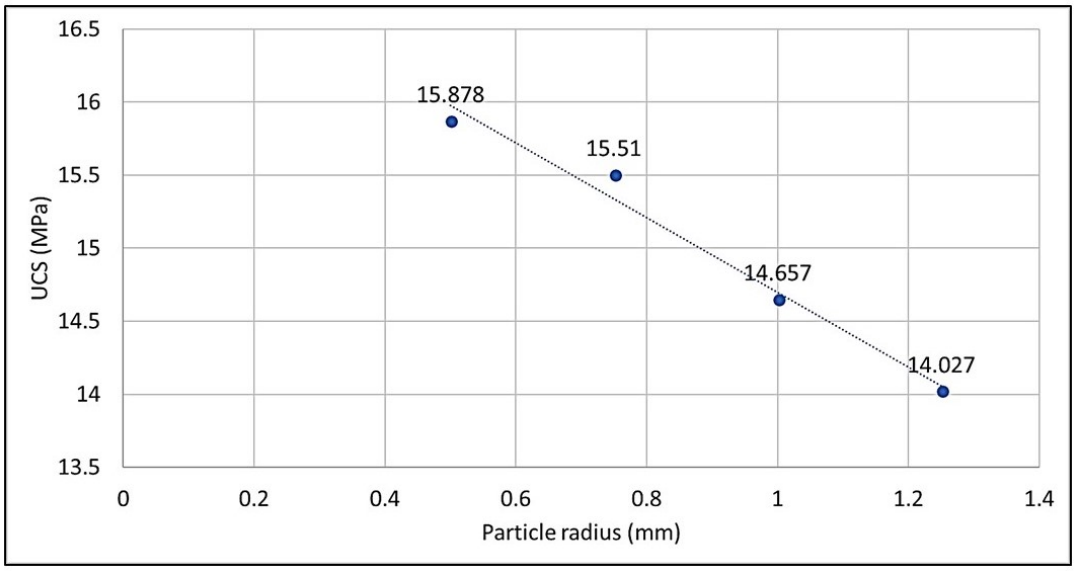

Figure 5.6: Effect of particle size on the UCS.

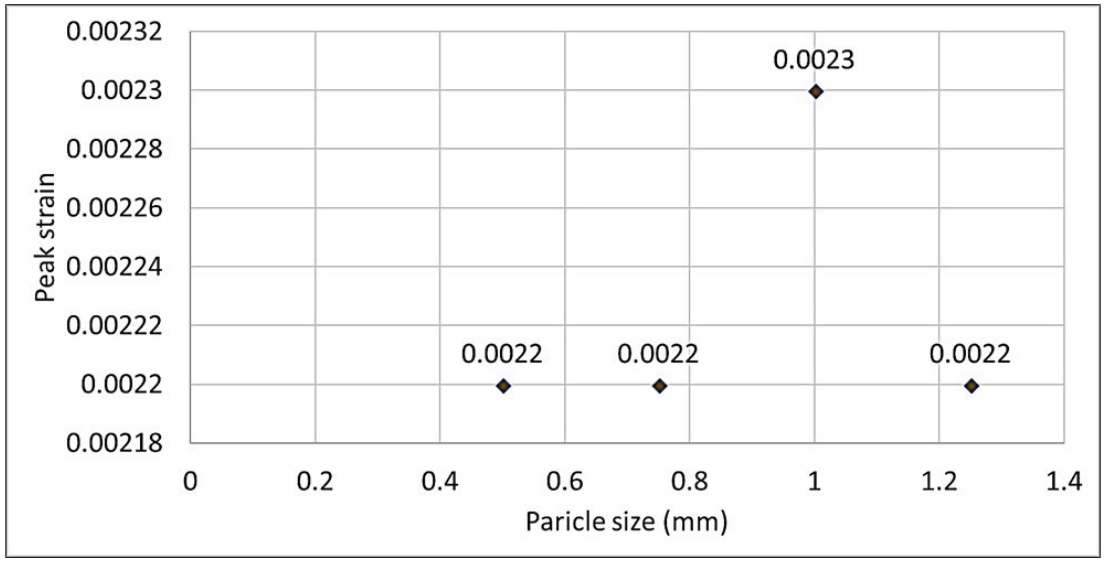

Figure 5.7: Effect of particle size on the peak strain.

5.3 Solution Parameter Set

As DEM is highly sensitive to input parameters, it is very likely to get more than one combination of input parameters to yield same numerical solution. Thus, in DEM modeling, there is no unique solution set of parameters to achieve the desired response of the material. In this section, it is shown that due to this flexibility provided in the

material model, a stress-strain response obtained for 1.0 mm particle can be adjusted so as to get close to the stress-strain response of 1.25 mm particle as shown in Fig 5.8.

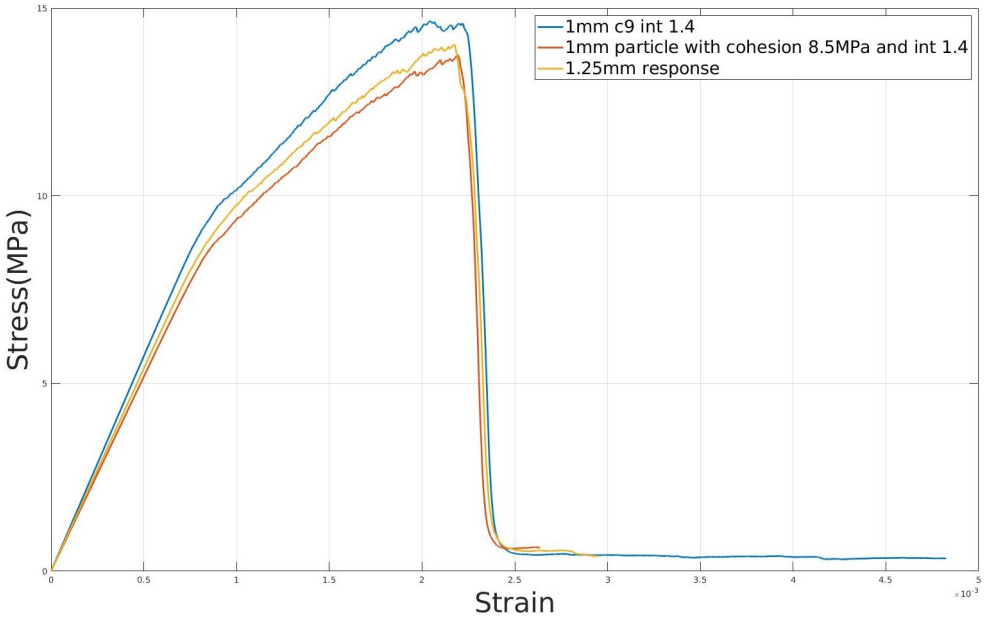

Figure 5.8: Material response for two different sizes of particles.

The blue coloured graph in the figure represents the material response for 1 mm particle and the yellow coloured graph represents the material response for 1.25 mm particle. It can be seen from the Fig 5.8 that the 1 mm particle response is brought closer to the 1.25 mm particle response by varying a couple of parameters. This flexibility offered by JCFPM is very convenient and helpful in reproducing or changing the material response according to the user input.

5.4 Influence Of Interaction Range

As described in chapter 4, unlike the classic material models where only discrete elements which are in direct contact are connected, JCFPM offers a parameter called interaction range. This feature provides the flexibility of adjusting the degree of interlocking of the discrete elements forming the numerical medium [6]. Bonds are connected between discrete elements if respective interaction ranges overlap each other.

By defining interaction range to be 1, the classic material model behavior can be obtained with this method. This is similar to clump particle logic proposed by Cho et al. (2007). However, this model has lesser computational complexity. The resulting medium consists of a packing where particles are not described by a unique contact anymore.

As interaction range is increased, more number of particles will be connected to each parent particle and overall interlocking of the packing will be increased. This should directly affect the force required for bond breakage and ultimately the ultimate compressive strength of the material should ideally be increased as shown in Fig 5.9.

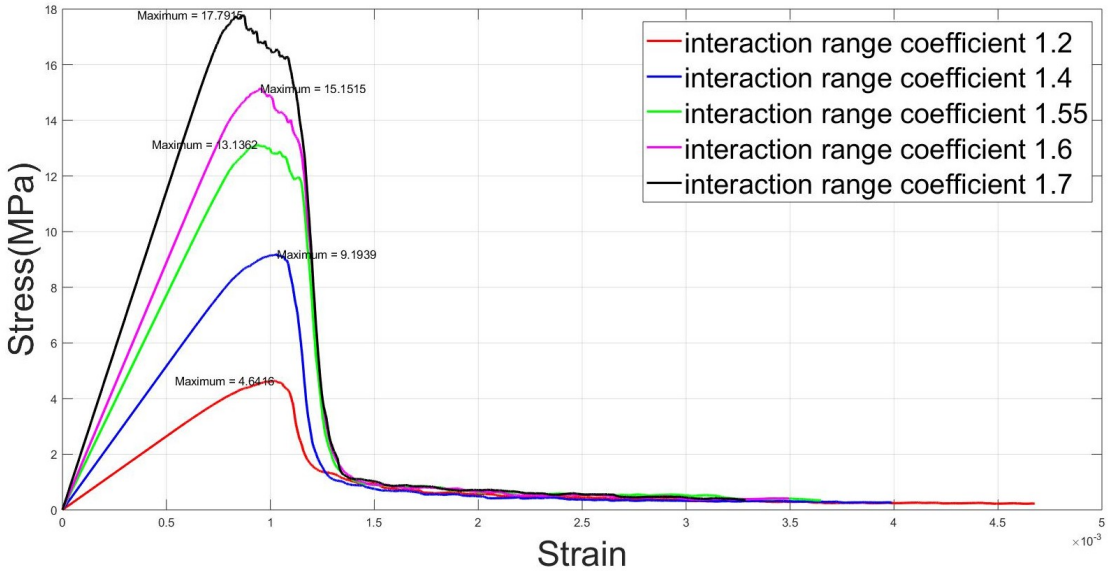

Figure 5.9: Influence of interaction range on material behavior.

These results are validated through the work of Scholtès and Donzé. They have presented similar effect of the interaction range on the behavior of the material.

5.5 Influence Of Cohesion

From the parametric study, it is observed that the value of cohesion affects the behavior of material in terms of both stress and strain response. As mentioned in the chapter 3, cohesion value directly affects the maximum shear force $F_{s,max}$ as,

$$F_{s,max} = F_n tan\phi_b + cA_{int} \tag{5.3}$$

Hence, as we increase the value of c, the value of $F_{s,max}$ increases. This implies that, larger force will be required to break the bonds between discrete element particles. The influence of the cohesion is shown in Fig 5.10.

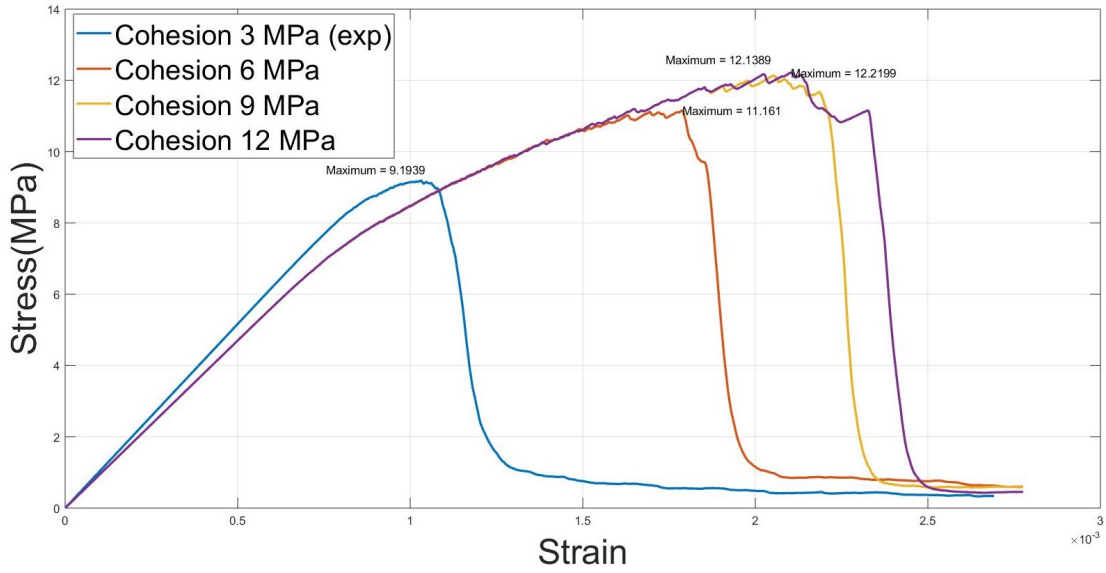

Figure 5.10: Influence of cohesion of material behavior.

From the obtained results, it can be seen that, as the cohesion value is increased the ultimate compressive strength as well as strain to failure is also increased.

5.6 Influence Of Particle Distribution Inside The Domain

Two different packing arrangements are used to study the effect of this parameter. Four different particle particle sizes are used for this study. For each size variation, the domain was filled with particles with random distribution packing and hexagonal distribution packing. The packing densities and response of the material behavior is studied for every case. Fig 5.11 and Fig 5.12 shows the packing variation between the two methods for 1 mm particle size.

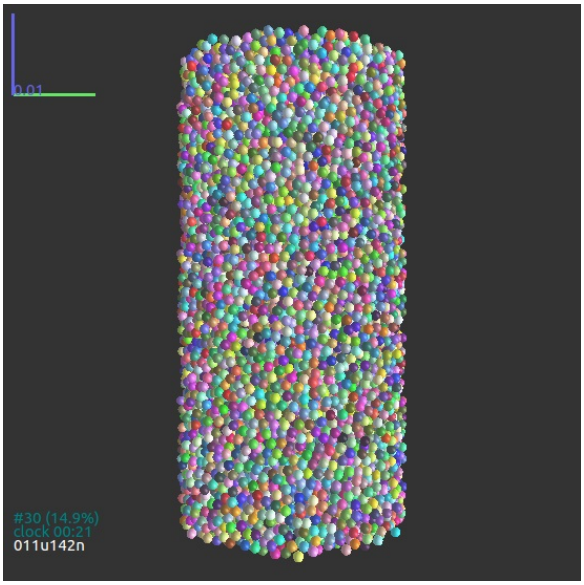

Figure 5.11: 1 mm particle with random distribution packing.

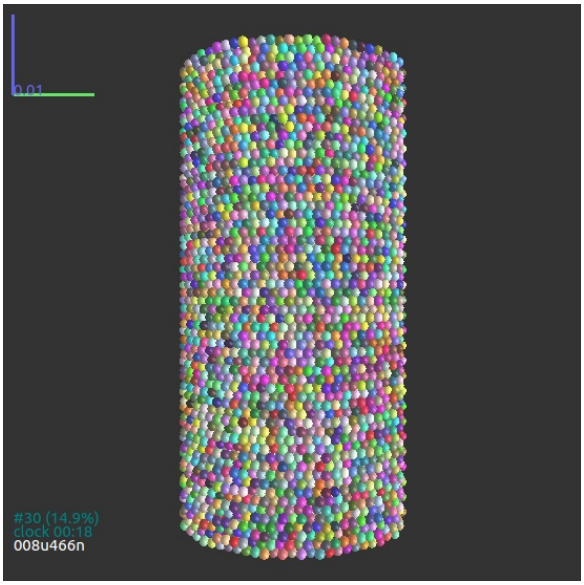

Figure 5.12: 1 mm particle with hexagonal distribution packing.

Fig 5.13 and Fig 5.14 shows the packing variation between two methods for 0.75 mm particle size

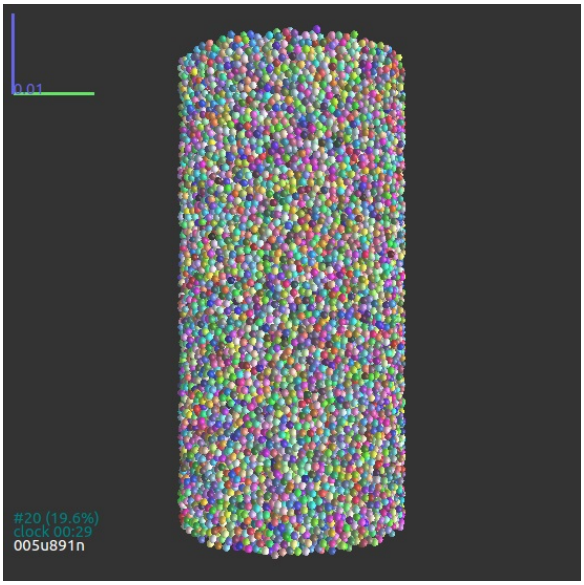

Figure 5.13: 0.75 mm particle with random distribution packing.

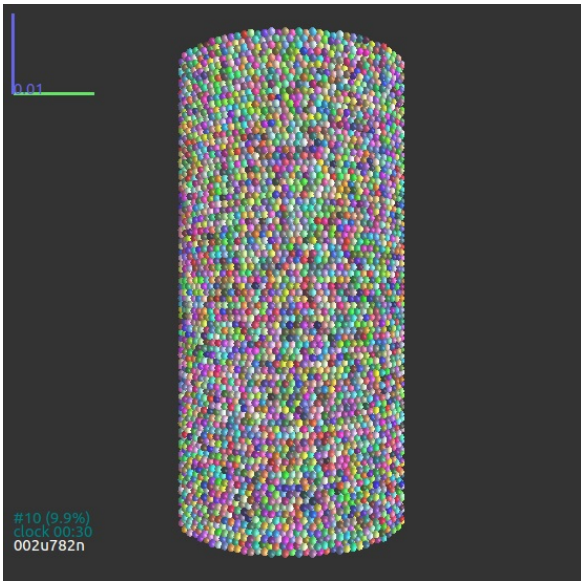

Figure 5.14: 0.75 mm particle with hexagonal distribution packing.

Fig 5.15 and Fig 5.16 shows the packing variation between two methods for 0.5 mm particle size

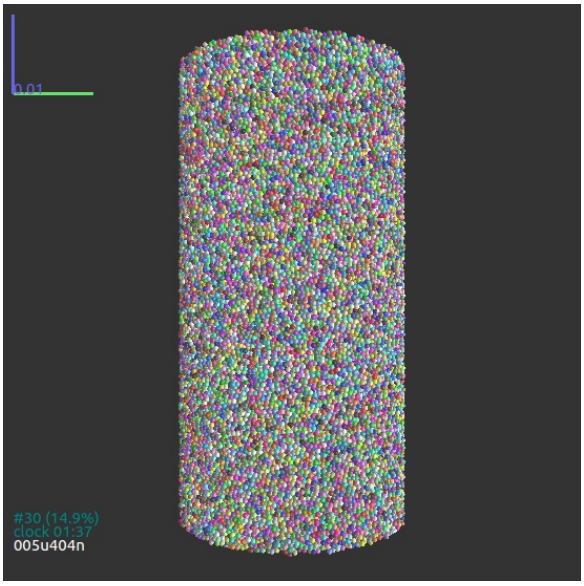

Figure 5.15: 0.5 mm particle with random distribution packing.

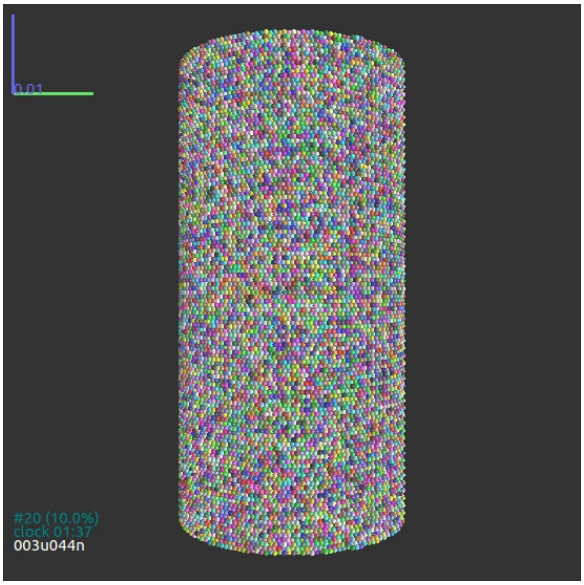

Figure 5.16: 0.5 mm particle with hexagonal distribution packing.

Above figures represent structure for various particle radii. To understand the effect more effectively, the stress-strain curve and packing densities need to be studied for this. Fig 5.17 & Fig5.18 shows the representation of the structure and Fig 5.20 shows the packing densities comparison for hexagonal packing and random distribution packing.

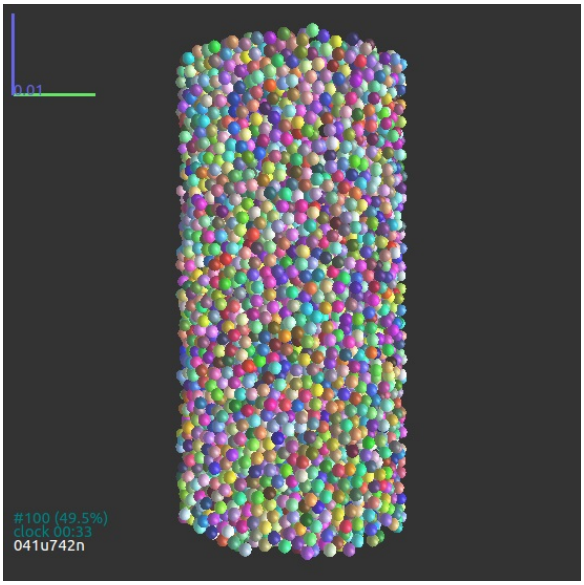

Figure 5.17: 1.25 mm particle with random distribution packing.

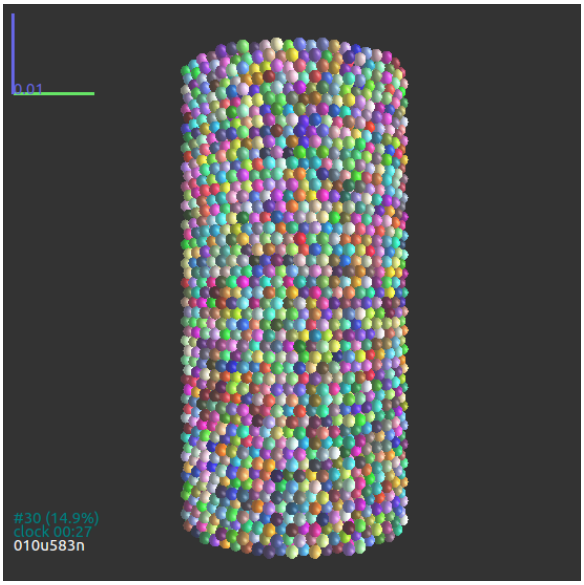

Figure 5.18: 1.25 mm particle with hexagonal distribution packing.

Following table 5.2 represents the values of packing densities for hexagonal packing and random packing for different particle sizes and Fig 5.19 provides the graphical representation of these densities.

Table 5.2: Comparison of packing densities between hexagonal and random distribution methods.

Particle size (mm)	Random distribution packing (%)	Hexagonal distribution packing (%)
0.25	53.5	72.2
0.5	52	70.19
0.75	50	67.97
1.0	49.2	66.2
1.25	48)	65

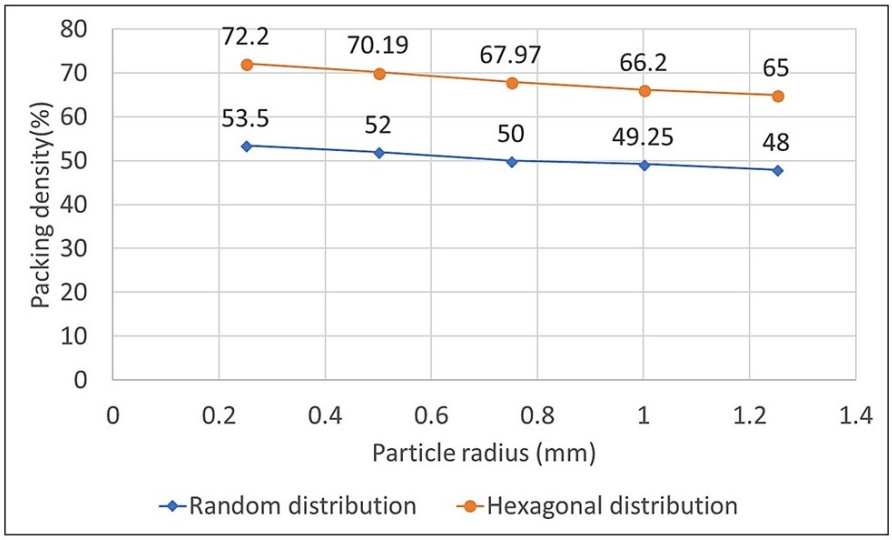

Figure 5.19: Packing densities for hexagonal and random packing.

As shown in Fig 5.20, hexagonal distribution of particles gives larger values of UCS and strain to failure. However, an abnormal peak is seen in the nature of the graph. This peak is undesirable and this result might not represent the accurate behavior of the system. Even though the values of UCS and strain to failure are lesser in case of random packing, the nature of the curve is smooth and these values can be adjusted to required values by adjusting the other parameters of the model.

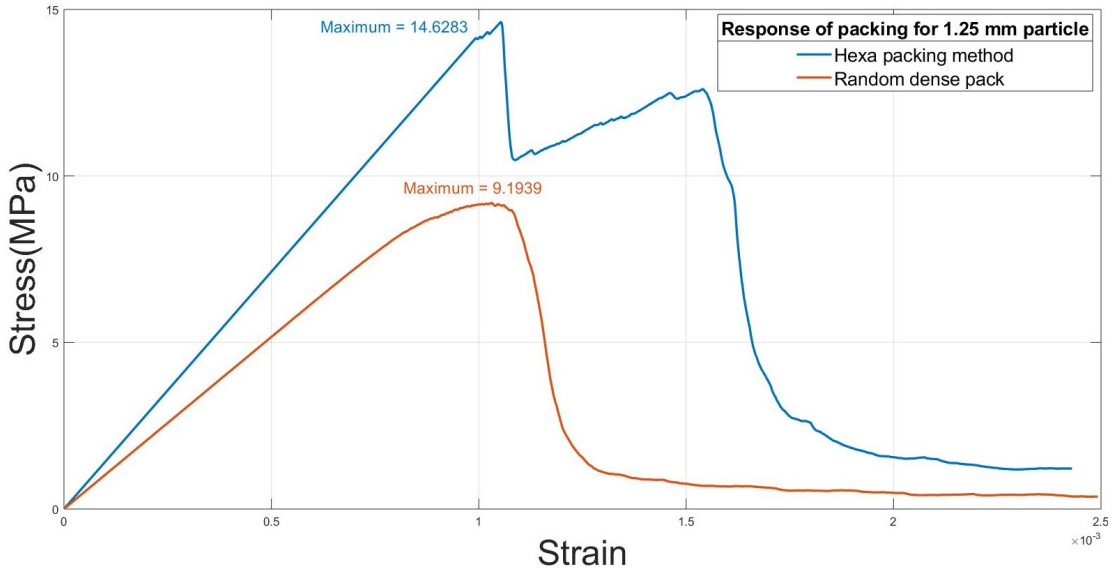

Figure 5.20: Material response for hexagonal and random packing.

5.7 Influence Of Particle Generation Method

In DEM, particle generation method has large influence on the response of the material. As stated in chapter 2, there are mainly three particle generation methods,

- Mono-disperse
- Bi-disperse
- Poly-disperse

In this study mono-disperse and poly-disperse generation methods are studied. In Yade, poly-disperse particle generation can be controlled by a parameter called fuzz. As per the user input of the fuzz value, DEM code evaluates and distributes the particles of different radii in the domain. Radius variation inside the domain is computed as follows.

$$Particle\ radius\ = initial\ particle\ radius\ \pm (initial\ particle\ radius \times fuzz) \quad (5.4)$$

Corresponding to the fuzz input, particles of all three dimensions as shown in equation 5.4 are generated inside the domain. The selection and distribution of these radii are random inside the domain. Following figures represent fuzz variation for 1.25 mm particle size.

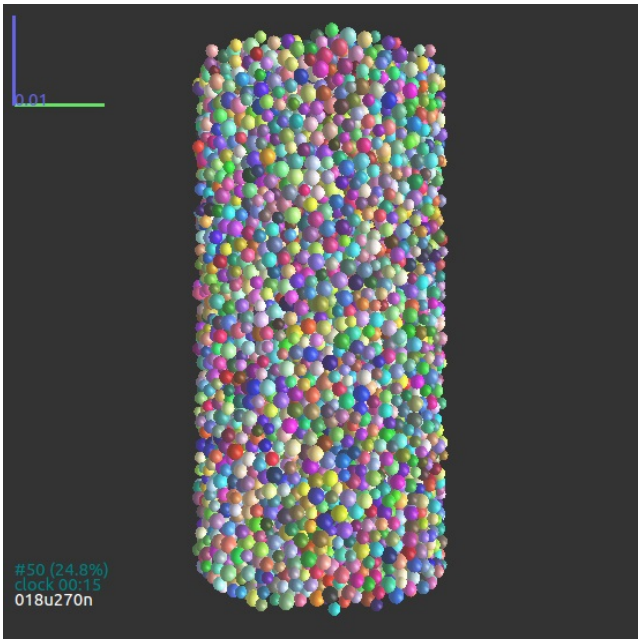

(a)

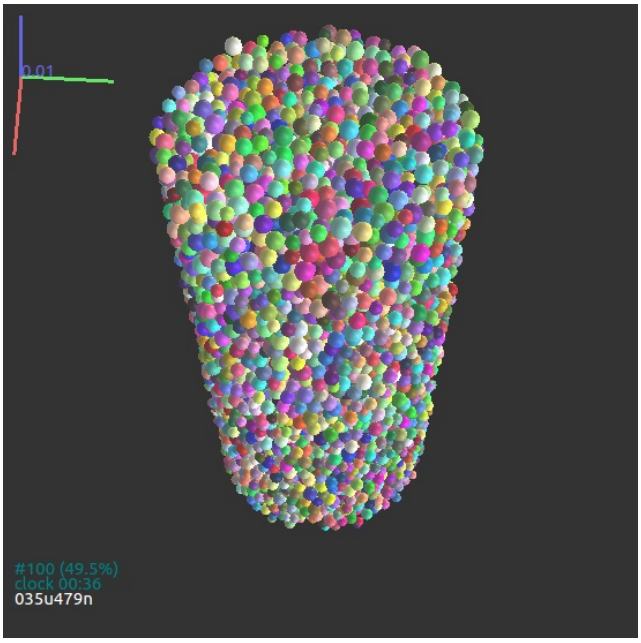

(b)

Figure 5.21: Fuzz variation coefficient 0.2

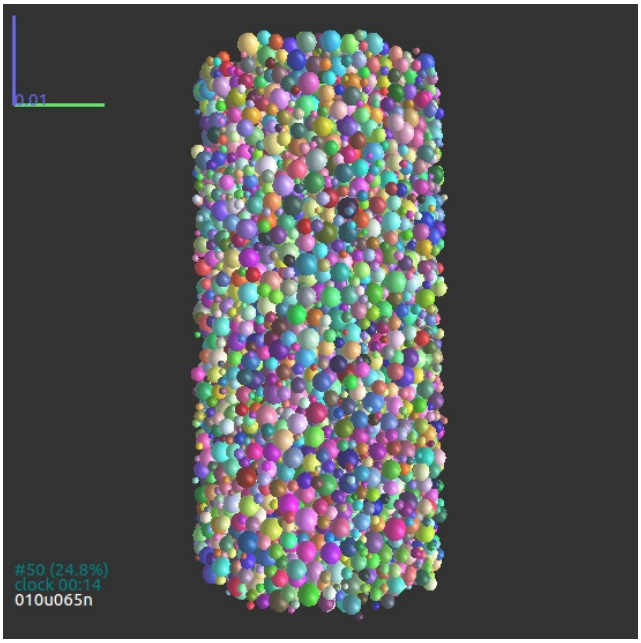

(a)

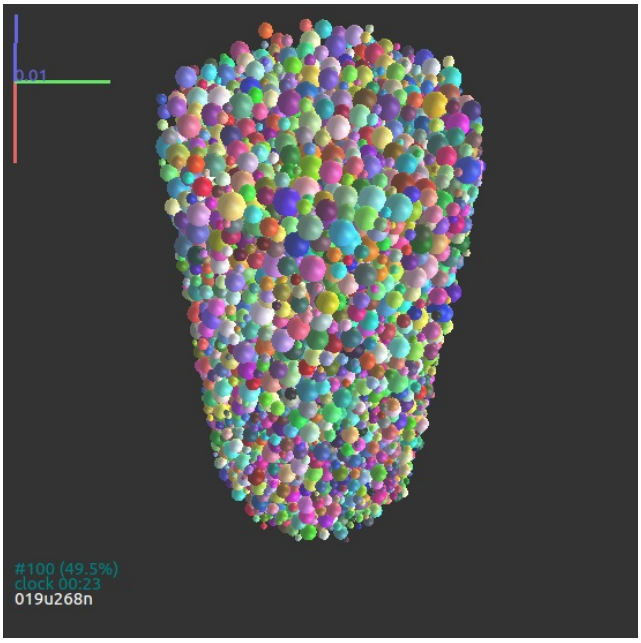

(b)

Figure 5.22: Fuzz variation coefficient 0.4

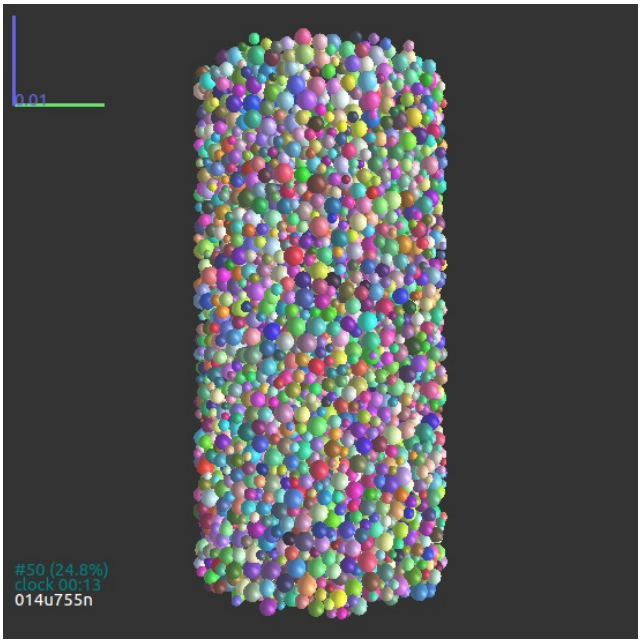

(a)

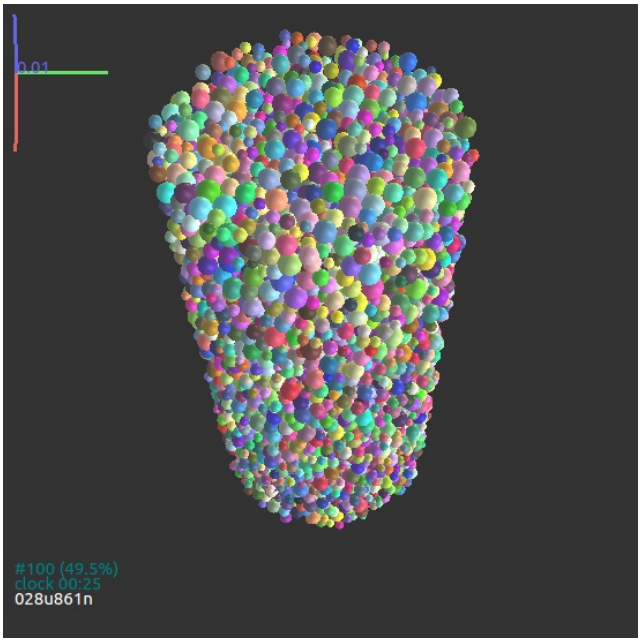

(b)

Figure 5.23: Fuzz variation coefficient 0.6

To understand the effect of poly-disperse particle generation method, each case of the fuzz variation is simulated with same DEM parameters used for 1.25 mm mono-disperse particle generation code. Following Fig 5.24 shows the effect of different fuzz

values on the behavior of material.

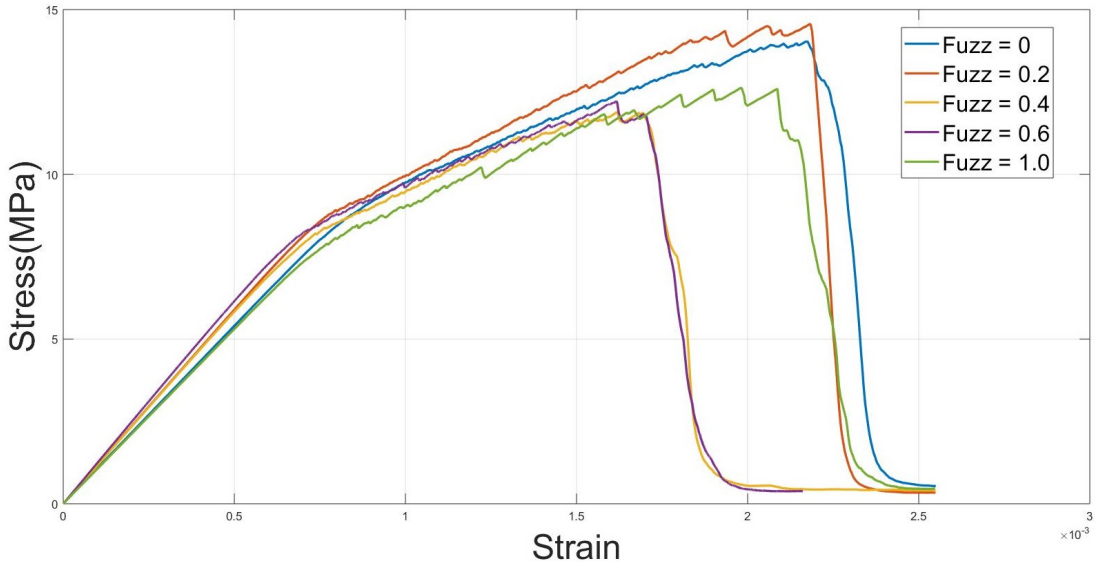

Figure 5.24: Material response for different poly-disperse particle generation algorithms.

As the fuzz coefficient is increased, the UCS and strain to failure decreases in all the other cases except for $fuzz = 0.2$. Further in-detail analysis needs to be performed to understand the mechanism behind this particular response.

CHAPTER 6: CONCLUSIONS AND RECOMMENDATIONS FOR FUTURE WORK

6.1 Conclusions

This chapter summarizes the results presented in this research work. With properly calibrated parameters, it can be concluded that JCFPM can be successfully used in DEM to model cementitious materials like plain concrete. Yade is the simulation tool used in this research, because it has the flexibility of particle generation and packing inside the domain which allows it to provide an accurate response of granular material behavior like concrete with less computational complexity. Yade is also computationally less expensive compared to other DEM packages. The simulation results obtained in this research work are in close agreement with the experiments performed by Flores and Pando [29].

As mentioned in the previous chapter, a parametric study including various micro and macro parameters was performed to calibrate DEM parameters in this research work. The implemented particle model in this study provides the accurate material response for plain concrete under a uniaxial compression test. From the results presented in this study, it can be concluded that the bulk response of the material depends upon the parameters such as, particle size, packing method, particle arrangement inside the domain, and material micro-properties. Due to the dependency of the model on parameters, care must be taken in deriving bulk properties of material based only on DEM simulations.

From the parametric study performed in this research work and results shown in section 5.3, it can be concluded that there is no unique set of parameters which gives accurate response in DEM. Therefore, validation of DEM models is important. As

there is no baseline for selection of parameter values in DEM, it opens the scope for future work to understand the optimal range of parameter values so that models can be accurately use to show bulk response of the material.

6.2 Recommendation For Future Work

The current research work demonstrates the modeling of a uniaxial compression response of a plain concrete using jointed cohesive friction particle model method. This research focuses on the unconfined loading conditions for concrete and the influence of model parameters on the response. However, there are several areas in this model which would need to be studied furthermore.

Parameter variation in this research was limited to five DEM parameters and their response on the material behavior. Further studies on influence of other parameters like modulus of elasticity, poisson's ratio and friction angle would help to understand the behavior in more detail.

Particle distribution in this study was limited to spherical particles. However, in physical material the particles are not exactly spherical. To model this, other shapes and combinations of shapes for particles need to be studied further. Also, response of poly-disperse method was studied at very preliminary stages. More simulations and detailed study need to be done in this particle generation method. If carefully designed, poly-disperse method would provide more insights into the packing density of the domain. Ideally larger packing can be obtained by filling a particle with small radii into the gaps between two large sized particles. However, this hypothesis is also preliminary and more studies need to be done.

Another extension of this study would be to include hoop strain calculation and validate it using experimental data. Although the study only focused on unconfined compression, it needs to be extended to confined compression test using DEM as well as validated to gain a better understanding about material modeling using DEM.

REFERENCES

[1] H. Zhu, Z. Zhou, R. Yang, and A. Yu, "Discrete particle simulation of particulate systems: Theoretical developments," *Chemical Engineering Science*, vol. 62, no. 13, pp. 3378 – 3396, 2007. Frontier of Chemical Engineering Multi-scale Bridge between Reductionism and Holism.

[2] A. V. Potapov and C. S. Campbell, "The two mechanisms of particle impact breakage and the velocity effect," *Powder Technology*, vol. 93, no. 1, pp. 13 – 21, 1997.

[3] H. Kim and W. G. Buttlar, "Discrete fracture modeling of asphalt concrete," *International Journal of Solids and Structures*, vol. 46, no. 13, pp. 2593 – 2604, 2009.

[4] P. A. Cundall and O. D. L. Strack, "A discrete numerical model for granular assemblies," *Géotechnique*, vol. 29, no. 1, pp. 47–65, 1979.

[5] D. Potyondy and P. Cundall, "A bonded-particle model for rock," *International Journal of Rock Mechanics and Mining Sciences*, vol. 41, no. 8, pp. 1329 – 1364, 2004. Rock Mechanics Results from the Underground Research Laboratory, Canada.

[6] L. Scholtès and F. Donzé, "A dem model for soft and hard rocks: Role of grain interlocking on strength," vol. 61, pp. 352–369, 02 2013.

[7] S. Liu, D. Sun, and Y. Wang, "Numerical study of soil collapse behavior by discrete element modelling," *Computers and Géotechnics*, vol. 30, no. 5, pp. 399 – 408, 2003.

[8] M. Yao and A. Anandarajah, "Three-dimensional discrete element method of analysis of clays," vol. 129, 06 2003.

[9] T. Moon, M. Nakagawa, and J. Berger, "Measurement of fracture toughness using the distinct element method," *International Journal of Rock Mechanics and Mining Sciences*, vol. 44, no. 3, pp. 449 – 456, 2007.

[10] Q. Wang, S. Gao, B. Jiang, S. Li, M. He, H. Gao, and Q. Qin, "Rock-cutting mechanics model and its application based on slip-line theory," vol. 18, 05 2018.

[11] J. Rojek, "Discrete element modelling of rock cutting," 2007. Computer methods in material science, 7:224-230.

[12] D. Hallbauer, H. Wagner, and N. Cook, "Some observations concerning the microscopic and mechanical behaviour of quartzite specimens in stiff, triaxial compression tests," *International Journal of Rock Mechanics and Mining Sciences & Geomechanics Abstracts*, vol. 10, no. 6, pp. 713 – 726, 1973.

[13] B. Schneider, M. Bischoff, and E. Ramm, "Modeling of material failure by the discrete element method," vol. 10, pp. 685 – 688, 12 2010.

[14] V. Å milauer, "Yade documentation," 2018. 2nd Edition, The Yade Project. DOI 10.5281/zenodo.34073.

[15] P. Wang and C. Arson, "Discrete element modeling of shielding and size effects during single particle crushing," *Computers and Geotechnics*, vol. 78, pp. 227 – 236, 2016.

[16] F. K. Wittel, H. A. Carmona, F. Kun, and H. J. Herrmann, "Mechanisms in impact fragmentation," *International Journal of Fracture*, vol. 154, pp. 105–117, Nov 2008.

[17] M. Nitka and J. Tejchman, "Modelling of concrete behaviour in uniaxial compression and tension with dem," *Granular Matter*, vol. 17, pp. 145–164, Feb 2015.

[18] N. S. Tannu, "A discrete element approach to predicting the uniaxial compressive response of plain concrete," 2017.

[19] "Pfc dcumentation," 2018. Itasca consulting group.

[20] A. Lisjak and G. Grasselli, "A review of discrete modeling techniques for fracturing processes in discontinuous rock masses," *Journal of Rock Mechanics and Geotechnical Engineering*, vol. 6, no. 4, pp. 301 – 314, 2014.

[21] R. S. C. Ergenzinger and P. Eberhard, "A discrete element model to describe failure of strong rock in uniaxial compression," 2011. Granular Matter, 13(4):341-364.

[22] C. O'Sullivan, *Particulate Discrete Element Modelling: A Geomechanics Perspective*. Taylor & Francis, 2011.

[23] B. Mishra and R. K. Rajamani, "The discrete element method for the simulation of ball mills," *Applied Mathematical Modelling*, vol. 16, no. 11, pp. 598 – 604, 1992.

[24] J. Rotter, M. Holst, J. Ooi, and A. M. Sanad, "Silo pressure predictions using discrete-element and finite-element analyses," vol. 356, 11 1998.

[25] B. Regassa, N. Xu, and G. Mei, "An equivalent discontinuous modeling method of jointed rock masses for dem simulation of mining-induced rock movements," *International Journal of Rock Mechanics and Mining Sciences*, vol. 108, pp. 1 – 14, 2018.

[26] P. Moysey and M. Thompson, "Modelling the solids inflow and solids conveying of single-screw extruders using the discrete element method," *Powder Technology*, vol. 153, no. 2, pp. 95 – 107, 2005.

[27] P. A. Cundall and O. D. L. Strack, "A discrete numerical model for granular assemblies," *Geotechnique*, vol. 29, no. 1, pp. 47–65, 1979.

[28] Y.-C. Chung and J. Ooi, "Confined compression and rod penetration of a dense granular medium: Discrete element modelling and validation," pp. 223–239, 01 2006.

[29] O. Flores and M. Pando, "Triaxial experiments on plain concrete," *University of Puerto Rico at Mayaguez, Civil Engineering Research Center, Report CERC-08–010, 95 p.*, 2008.

[30] Z. Gyurkò, K. Bagi, and A. Borosnyòi, "Discrete element modelling of uniaxial compression test of hardened concrete," vol. 66, pp. 113–119, 01 2014.

[31] M. P. S. apfer, S. Abe, C. Childs, and J. J. Walsh, "The impact of porosity and crack density on the elasticity, strength and friction of cohesive granular materials: Insights from dem modelling," *International Journal of Rock Mechanics and Mining Sciences*, vol. 46, no. 2, pp. 250 – 261, 2009.

[32] R. Altindag and A. Guney, "Predicting the relationships between brittleness and mechanical properties (ucs, ts and sh) of rocks," vol. 5, 08 2010.

[33] F. Donze, J. Bouchez, and S. Magnier, "Modeling fractures in rock blasting," *International Journal of Rock Mechanics and Mining Sciences*, vol. 34, no. 8, pp. 1153 – 1163, 1997.

[34] R. Hart, P. Cundall, and J. Lemos, "Formulation of a three-dimensional distinct element model part ii. mechanical calculations for motion and interaction of a system composed of many polyhedral blocks," *International Journal of Rock Mechanics and Mining Sciences & Geomechanics Abstracts*, vol. 25, no. 3, pp. 117 – 125, 1988.